finding suggests that other factors regulate HSC generation from human ES cells.

Importantly, Niwa et al. report that a novel serum-free monolayer culture system, independent of OP9 feeder cells and EB formation enables hematopoietic differentiation from both ES (KhES1) and iPS (201B7, 253 G4) cells. Using the method, the investigators generated $CD34^+CD45^+$ HPCs from human KhES1 between culture days 10 to 25 [17]. Tolar et al. reported hematopoietic differentiation of iPS cells from patients with mucopolysaccharidosis (MPS) type I, which is treated via HSC transplantation. An EB-mediated method generated HPCs expressing CD34 and CD45 and HSCs expressing *CD34* and *CD38* mRNA [20]. It is now necessary to determine whether HPCs derived from gene manipulation-free methods can have repopulation capacity in vivo.

Erythroid Cells

Red blood cells (RBCs), which are differentiated from erythroid progenitors (BFU-E, CFU-E) and erythroblasts, deliver oxygen (O_2) to the body tissues. Pluripotent cell-derived erythroid cells could be utilized as blood products in future clinical applications. It is not yet known whether erythroid cells derived from ES and iPS cells are definitive (EryD), enucleate, generate adult type of hemoglobin or carry oxygen (Fig. 3). In mouse, ES-derived cells co-cultured with OP9 cells contain primitive erythroid cells (EryP) within 8 days and erythroid progenitor cells (EryD) in 10 when cultured in methylcellulose semi-solid culture in the presence of Epo and IL-3. $Ter119^+$ cells were generated in the same condition after 14 days [28–30]. Within 5–6 days, EB culture-derived cells contain erythroid progenitor cells in methylcellulose culture in the presence of Epo and SCF, and those cells show a peak of *βH1 globin*, *βmajor globin* and *Gata1* gene expression within 7–8 days of culture [31].In addition to co-culture and EB formation methods, a three-step differentiation method is highly efficient in inducing erythroid cells from ES cells [32]. After 6 days of EB culture, ES-derived erythroid cultures (ES-EPs), which contain $CD71^+$c-$Kit^+Ter119^+$proerythroblasts and *βmajor globin*-expressing definitive erythroid cells, are induced with Epo, SCF, dexamethasone (Dex), insulin-like growth factor (IGF)-1. Following that, Epo, insulin, glucocorticoid receptor antagonist and transferrin were added to induce hemoglobinized, enucleated RBCs from ES-EP cells that also differentiate into $Ter119^+$ cells in vivo [32]. Hanna's group reported that after 6 days of culture on OP9 stromal cells, mouse autologous iPS cells, which were established from fibroblasts from a sickle cell anemia model, gave rise to c-Kit^+CD41^+ early HPCs in vitro and that HPCs derived by EB formation could rescue anemia in vivo after transplantation [25]. This work suggested that similar strategies are possible in humans.

Human ES cells co-cultured with mouse fetal liver-derived stromal cells (mFLSCs) generated erythroid progenitors after day 10, dominantly express adult type β-globin rather than embryonic type ε-globin, and gradually enucleate and show oxygen saturation around day 16 [33]. Lu et al. report that functional oxygen-carrying erythrocytes can be prepared on a large scale (10^{10}–10^{11} cells per 6-well plate of human ES cells) using four culture steps. They are: Step1; EB formation and hemangioblast precursor induction with BMP4, $VEGF_{165}$, bFGF, SCF, TPO and Flt-3 L (days −3.5 to 0); Step2; hemangioblast expansion with bFGF and tPTD-HoxB4 fusion protein (days 0 to10); Step3; erythroid cell differentiation and expansion with EPO (days 11 to 20); and Step4; enrichment of erythroid cells (day21) [34]. Human fibroblast-derived cell lines, such as hFib2-iPS5, 201B6, 201B7, 253G1 and 253G4, and the bone marrow mesenchymal stem cell-derived MSC-iPS1 cell line, all established from healthy donors, produced erythroid cells at around 30 days of culture via either EB formation or co-culture with OP9 stromal cells [17–19, 35]. On the other hand, two groups reported that human iPS cells from patients with hematological diseases also differentiated into erythroid cells. A combination method using EBs and OP9 cells produced BFU-E progenitor cells from dermal fibroblast-reprogrammed iPS cell lines, which were established from patients with Fanconi anemia (FA) [36]. Human peripheral blood-reprogrammed iPS cells established from patients with polycythemia vera (PV), a myeloproliferative disorder, also differentiate into CFU-E and $CD45^-$/CD235a $(GPA)^+$ mature erythroid cells after 2–3 weeks of EB formation, followed by culture of EB-derived $CD34^+CD45^+$ cells with SCF, IL-3. EPO [37].

Megakaryocytes and Platelets

Platelets, which are derived from fragmentation of precursor megakaryocytes, play a pivotal role in hemostasis by aggregation and adhesion to subendothelial tissue. In terms of regenerative medicine, pluripotent cell-derived platelets could be utilized as blood products in clinical settings. As an experimental tool, pluripotent cell-derived megakaryocytes could be useful to explore signaling pathways utilized in platelet formation, as a genetic approach has limited utility in studying anucleated platelets. One question is whether cells derived from ES and iPS cells would express surface antigen marker, such as CD41 andCD61, have the same signal pathway, exhibit the same morphology and have the same aggregation and adhesion capacity as megakaryocytes and platelets in vivo (Fig. 4).

In mice, Era et al. first reported that megakaryocytes derived from ES cells were observed 8 days after co-culture with OP9 cells and TPO [38].Co-culture of ES cells with OP9

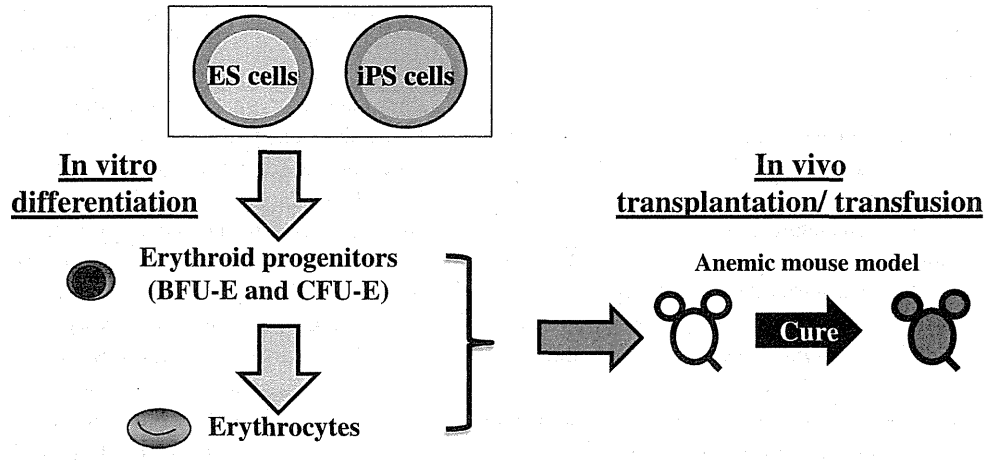

Cell type	Surface markers		Specific genes		Other characteristics
	Mouse	Human	Mouse	Human	
Erythrocytes	Ter119	GPA	*Gata1* *Eklf* *βH1–globin* *β major-globin*	*GATA1* *EKLF* *β-GLOBIN*	1) Oxygen-carrying capacity 2) Improvement the anemic status by transplantation and transfusion (In vivo)

Fig. 3 Schematic diagram of pluripotent cell- derived erythrocytes. ES and iPS cells-derived erythrocytes are characterized by the expression of erythroid surface markers (Ter119 in mouse; Glycophorin A in human) and specific transcription factor genes (*Gata1, Eklf, βH1-globin* and *β−major globin* in mouse; *GATA1, EKLF* and *β-GLOBIN* in human). Hemoglobins in erythrocytes function as an oxygen-carrier and can be evaluated by plotting the oxygen equilibrium curves. To further investigate the function of erythrocytes in vivo, erythrocytes are transplanted/transfused into anemic mouse model. BFU-E; Burst Forming Unit-Erythroid, CFU-E; Colony Forming Unit-Erythroid, GPA; Glycophorin A

stromal cells for 8–12 days in the presence of TPO, IL-6 and IL-11 resulted in development of large, polyploid megakaryocytes, which produce proplatelets, could bound fibrinogen after exposure to platelet agonists, and exhibited integrin-mediated megakaryocyte signaling [39]. Fujimoto et al. confirmed primitive and definitive megakaryopoiesis from mouse ES cells with OP9 stromal cells in the presence of TPO. At the same time, $CD41^+$ platelets were generated in the culture supernatant via two waves of differentiation. ES-derived platelets of the definitive wave are similar in structure to those in peripheral blood and exhibit fibrinogen-binding ability and CD62P (P-selectin) expression after addition of AYPGFK, a platelet agonistpeptide [40].

In humans, 17 days after human H1 ES-derived cells on mouse bone marrow S17 cell lines contained megakaryocyte progenitor cells (CFU-Mk) that expressed CD41 antigen [41]. Gaur et al. reported that human H9 ES-derived cells grown on OP9 cells also generate megakaryocytic cells after 15–17 days of culture with TPO. CD41-, CD42b- and von Willebrand factor (vWF)-expressing megakaryocytes were polyploid (2 N to 32 N) and responsive to integrin $\alpha_{IIb}\beta_3$ activation by agonists such as ADP and PAR1 [42]. Takayama et al. reported a modified method of OP9 co-culture useful to produce not only megakaryocytes but also functional platelets. Differentiated ES cells co-cultured on OP9 or 10 T1/2 cells (a mouse embryonic mesenchymal stem cell line) with VEGF for 14–15 days formed embryonic stem cell-derived sacs (ES-sacs), which consist of multiple cysts that retain properties of endothelial cells and express CD34, VE-cadherin, CD31, CD41a, and CD45. After 9–10 days culture of ES-sacs with TPO, IL-6, IL-11, SCF and heparin, cultures produced functional platelets [43]. The same group succeeded in inducing platelets through "iPS-sacs" from human iPS cell lines reprogrammed from healthy adult human dermal fibroblasts [44].

Macrophages

Macrophages, which are differentiated from monocytes, are amoeboid cells that function in both innate immunity and adaptive immunity, phagocytize bacteria, viruses and dead cells, and stimulate lymphocytes and other immune cells to respond to pathogens. Monocytes and macrophages play a critical role in initiation and progression of atherosclerotic lesions. Therefore, pluripotent cell-derived macrophages could be used in vitro as an experimental tool to clarify the mechanisms of atherosclerotic lesions. It is not known whether macrophages derived from pluripotent cells express

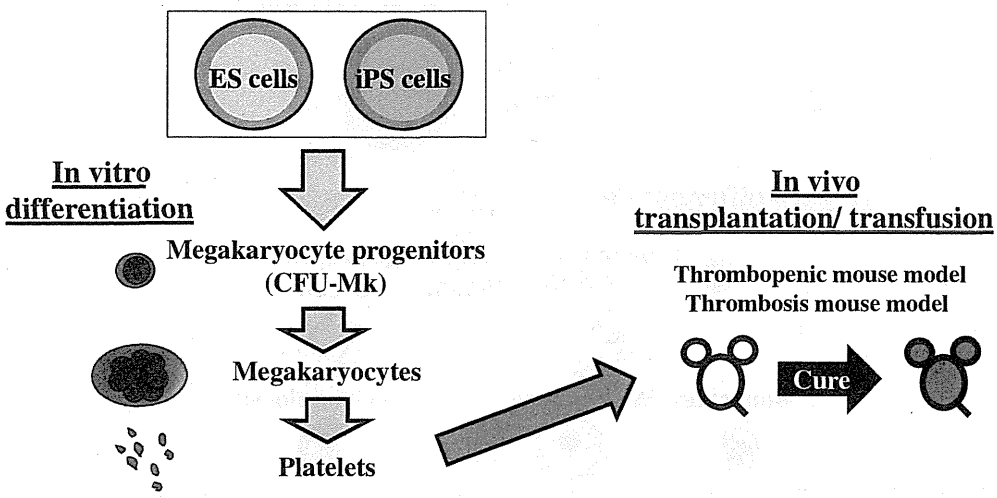

Cell types	Surface markers	Specific genes	Other characteristics
Megakaryocytes	CD41, CD42 CD61	*NF-E2* *FOG-1, Fli-1*	1) DNA ploidy 2) Aggregation and adhesion capacity
Platelets	CD41, CD42 CD61, CD62P	—	1) Aggregation and adhesion capacity 2) Thrombus formation to blood vessel injury (In vivo)

Fig. 4 Schematic diagram of pluripotent cell-derived megakaryocytes and platelets. ES and iPS cells-derived megakaryocytes are characterized by the expression of megakaryocyte surface markers (CD41, CD42 and CD61 in both mouse and human) and specific transcription factor genes (*NF-E2, FOG-1* and *Fli-1* in both mouse and human). DNA ploidy, a representative characteristic of megakaryocytes is examined in CD41 positive cells. Aggregation and adhesion capacity, another characteristic of megakaryocytes, are examined by fibrinogen binding assay and the integrin alpha II beta 3 signaling pathway. ES and iPS cells-derived platelets are characterized by the expression of surface markers (CD41, CD42, CD61 and CD62P in both mice and human). To further investigate the function of platelets in vivo, platelets are transplanted/transfused into thrombopenic mice and injury-induced mice models, in which the improvement of its status and hemostasis can be evaluated, respectively. CFU-Mk; Colony Forming Unit-Megakaryocyte

appropriate cell surface antigen markers, such as CD11b and F4/80, exhibit similar gene expression patterns as normal macrophages, or show phagocytotic activity (Fig. 5).

In mice, 13–15 days after EB formation by ES cells (CCEG2 and D3) in the presence of Epo, IL-1, IL-3, and M-CSF, HCs containing macrophages are generated [45]. Co-culture on OP9 cells with ES (D3) cells for 10 days also induced macrophage progenitors in the presence of IL-3 and Epo [28]. In these reports, macrophages were confirmed by morphologically. Lindmark et al. found that ES-derived macrophages are more similar to those in the peritoneum than mouse macrophage cell lines (J774.A1 and RAW264.7) by DNA microarray analysis [46]. After 10–12 days of culture, ES (J1) cells formed EBs in methylcellulose in the presence of CSF-1 and IL-3. After 3–5 days of liquid culture with CSF-1 and IL-3, differentiated cells expressed F4/80, FcγRII, scavenger receptor A (SR-A), CD36 and CD68, exhibited phagocytosis, and secreted TNF-α and IL-6 in response to an inflammatory stimulus [47], suggesting ES cell-derived macrophages could be an appropriate model to study atherosclerosis-related macrophages. Senju et al. reported that F4/80- and CD11b- expressing macrophages from the mouse iPS cell line 38C-2, which was established from MEFs with Oct3/4, Sox2, Klf4, and c-Myc, were generated via co-culture with OP9 cells for 6 days without cytokines and for the next 6 days with GM-CSF, followed by feeder free culture with M-CSF. iPS-derived macrophages also showed complement C5a-induced chemotaxis, phagocytic capacity and produced nitric oxide after stimulation with LPS and IFN-γ [48].

In humans, 17 days after human H1 ES-derived cells on mouse bone marrow S17 cell lines contained macrophage progenitor cells (CFU-M) that expressed CD15 antigen [35, 41]. Human ES cell lines, such as KhES-1, KhES-3, H1 and HES2, and human fibroblast-derived cell lines, such as hFib2-iPS5, 201B7 and 253G4 and the bone marrow mesenchymal stem cell-derived MSC-iPS1 line, all established from healthy donors, contained CFU-Ms and produced $CD14^+$ monocytes, $CD11b^+$ macrophages (at day14–22) and $CD13^+$ myeloid cells (at day 30) after culture via EB formation or co-culture with OP9 stromal cells in the presence of cytokines [17, 19, 35].

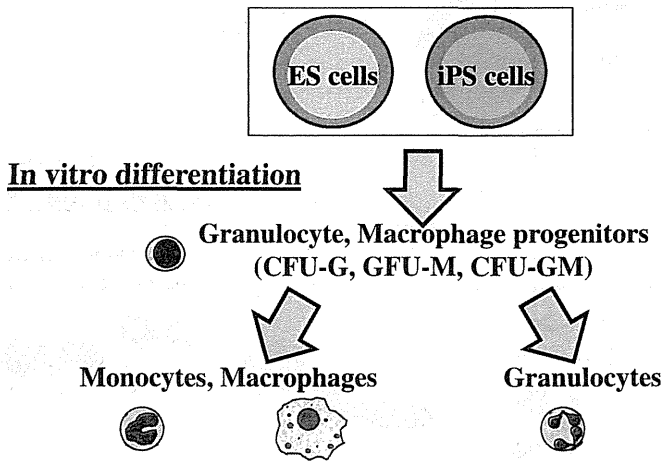

Cell types	Surface markers		Specific genes		Other characteristics
	Mouse	Human	Mouse	Human	
Monocytes Macrophages	CD11b, CD14, F4/80	CD11b, CD13, CD14, CD15, CD18	*MMP-3* *MMP-9*	*PU.1*	1) Phagocytotic capacity 2) Cytokine production
Granulocytes	Gr-1	CD11b, CD13, CD16, CD33	*PU.1*	*PU.1, MPO, CEBPα Lactoferrin Gelatinase*	1) Superoxide production 2) Chemotactic capacity

Fig. 5 Schematic diagram of pluripotent cell-derived monocytes, macrophages and granulocytes. ES and iPS cells-derived monocytes and macrophages are characterized by the expression of surface markers (CD11b, CD14 and F4/80 in mouse; CD11b, CD13, CD14, CD15 and CD18 in human) and specific transcription factor genes (*Metalloproteinase (MMP)-3* and *MMP-9* in mouse; *PU.1* in human). A representative characteristic of macrophages is phagocytotic capacity, in which fluorescence-conjugated *Escheria coli* is administered and its incorporation into macrophages is evaluated by in vitro culture. Also, macrophages can produce cytokine (interleukine-6 and tumor necrosis factor) in response to inflammatory stimulus, such as lipopolysaccharide. ES and iPS cells-derived granulocytes are characterized by the expression of surface markers (Gr-1 in mouse; CD11b, CD13, CD16 and CD33 in human) and specific transcription factor genes (*PU.1* in mouse; *PU.1, Myeloperoxidase (MPO), CEBPα, Lactoferrin* and *Gelatinase* in human). The representative characteristics of granulocytes are superoxide production in response to phorbolmyristate acetate (PMA) stimuli, and chemotactic capacity in response to the chemo-attractant in vitro. CFU-G; Colony Forming Unit-Granulocyte, CFU-M; Colony Forming Unit-Macrophage, CFU-GM; Colony Forming Unit-Granulocyte Macrophage

Granulocytes

Granulocytes, which are derived from common myeloid progenitors and myeloblasts and account for approximately 60 % of leukocytes, are composed of neutrophils, basophils and eosinophils. They contain cytoplasmic granules and play a pivotal role in immunesystem by consuming bacteria and dead cells. Decreases in the number of neutrophils promote infection in several pathological situations, such as leukocyte function deficiencies or myelosuppression caused by chemotherapy. Granulocyte transfusion therapy is considered effective for infections unresponsive to conventional antimicrobial therapies in severely neutropenic cancer patients. Therefore, pluripotent cell-derived neutrophils could be used for such procedures. Thus it is important to determine whether neutrophils derived from pluripotent cells express appropriate markers and exhibit behaviors such as chemotaxis and phagocytosis (Fig. 5).

Leiber et al. reported that mouse CCE ES cell-derived neutrophils are generated after 8 days of EB culture, followed by 7 days of co-culture with OP9 cells and cytokines. The co-culture system is more effective in enhancing the number and culture period of neutrophils produced from ES cells compared to methods that do not employ OP9 stromal cells. Those neutrophils are positive for the surface marker Gr-1, have granules containing lactoferrin and gelatinases, and exhibit chemotactic responses and superoxide production [49].

Several groups have reported neutrophil induction from human ES cells. EB formation of human KhES cells grown in the presence of OP9 cells and cytokines gives rise to CD15-, CD11b- (both neutrophil and monocyte markers) and CD16- (mature neutrophil marker) positive cells at day13 similar to neutrophils found in peripheral blood. They also exhibit the oxidative burst function in killing microorganisms and phagocytotic activity in vitro [50]. Saeki et

al. developed feeder free culture systems for neutrophil induction. ES-derived neutrophils were generated after 3 days of "sphere formation" culture of KhES-3 ES cells on low-attachment dishes in the presence of cytokines, followed by culture on gelatin-coated dishes up to 40 days, results similar to those reported by Yokoyama's group [51]. Choi et al. succeeded in expanding neutrophils from human ES cells at least 60 times more efficiently than previously reported. Their culture system employed three steps, including induction of $CD34^+/CD45^+$ HPCs for 9 days on OP9 cells, expansion of HPCs for 2–8 days without OP9 cells, and differentiation of HPCs for 8 days on OP9 cells plus G-CSF. In addition, a similar method is reportedly useful for human iPS cell lines established from neonatal foreskin and adult fibroblasts [52]. Morishima et al. analyzed the differentiation process and function of iPS-derived neutrophil in greater detail. Expression of *PU.1*, *CEBPα*, *MPO*, *lactoferrin*, and *gelatinase* was confirmed during induction, as was chemotactic activity, phagocytotic activity, and MPO chlorination activity was observed in neutrophils derived from 201B6, 253G1, 253G4 iPS cell lines, all of which were established from healthy dermal fibroblasts [18].

Recently, Zou's group reported that culture on OP9 stromal cells of human autologous iPS cells established from bone marrow mesenchymal stem cells from a patient with X-linked chronic granulomatous disease (X-CGD) gave rise to oxidase-deficient neutrophils. They were also successful in rescuing oxidase-deficiency by gene modification using zinc finger nuclease-mediated safe harbor targeting [53]. These findings demonstrate that precise gene targeting may be applied to correct a disease-causing mutation in patient iPS cells.

Lymphocytes

Lymphocytes, which consist of small lymphocytes (T cells and B cells) and large granular lymphocytes (NK cells), determine the specificity of immune response to infectious microorganisms and foreign substances. A decrease in lymphocyte number results in serious infections in several pathological situations, such as leukocyte function deficiencies or myelosuppression caused by chemotherapy. Immunotherapy for cancer is considered to be effective for cancer patients in clinical settings. Therefore, antitumor lymphocytes derived from pluripotent stem cells may be applicable to these approaches. It becomes the focus whether lymphocytes-derived from pluripotent cell express the surface antigen marker, achieve rearrangement of T cell antigen receptor (TCR) in T cell and immunoglobulin (Ig) in B cell and function such as cytotoxity (Fig. 6).

In mice, Nakano et al. reported that ES cells co-cultured on OP9 cells with IL-7 generated $B220^+$ early B cells, which were almost all IgM^- and achieved diversity-joining gene rearrangement, although a small portion of the hematopoietic cluster differentiated into mature IgM^+ cells expressing the complete μ chain mRNA [28]. B cell maturation from ES cells was enhanced in the presence of IL-7 and Flt3-L. Treatment with LPS stimulated B cell maturation and IgG secretion [54]. B cell differentiation from mouse iPS cells via the OP9 method revealed differences in outcomes according to iPS cell origin. MEF-derived iPS cells differentiated into B cells; however, B cell-derived iPS cells were relatively resistant to B cell lineage differentiation and showed defective Pax5 expression in differentiated cells [55].

Human H1 and H9 ES cell-derived $CD34^+$ cells co-cultured with MS-5 stromal cells in the presence of IL-3, IL-7, SCF and Flt3-L generated B cells positive for CD19 and for mRNA encoding the pre-B receptor complex (*VpreB*, *Igα*) [56]. Carpenter et al. first reported B cell lymphopoiesis from human iPS cells. $CD45^+CD19^+CD10^+$ cells-derived from iPS cells also expressed *Pax5*, *IL7αR*, *λ-like* and *VpreB receptor* mRNA. $CD45^+CD19^+$ cells exhibited multiple genomic D-J (H) reárrangements suggestive of pre-B-cell status [57].

T cell induction from ES cells has rarely been successful, due to difficulties in recapitulating the thymic stromal environment. de Pooter et al. reported that low population of $CD4^+$ and $CD8^+$ thymic subsets were generated from mouse ES cells as a result of co-culturing on OP9 cells, followed by $Flk1^+CD45^-$HPCs generated on fetal thymic organ cultures (FTOCs) [58]. They also developed modified OP9-DL1, which sustained mature T cells that expressed γδ and αβ TCRs, were positive for CD8, and produced IFN-γ in response to stimulation [59]. The OP9-DL1 method was also useful for mouse iPS differentiation. iPS-derived T cells secreted IL-2 and IFN-γ in response to in vitro stimulation and could also reconstitute T cell pools in Rag-deficient mice, suggesting that they follow a normal T cell differentiation program [60].

Galic et al. reported T-cell differentiation from human ES cells. Resulting differentiated H1 ES cells-derived progenitors grown in the presence of OP9 stromal cells for 10 to 19 days in vitro engrafted into human thymic tissues in immunocompromised mice. T cell development was observed in the conjoint organ 3–5 weeks after transplantation, indicating that human ES cells could be used to treat T cell disorders [61]. EB-derived T cell progenitors also generate to phenotypically and functionally normal cells of the T lineage when transferred into human thymic tissue implanted in immunodeficient mice [62]. Moreover, Timmermans et al. reported that during differentiation of ES cells on OP9 cells, two-dimensional structures form that strongly resemble blood islands, which arise during normal embryonic development and consist mostly of $CD34^+$ cells. Sequential culture of ES cell-derived cells on OP9-DL1 monolayers produced $CD34^{high}CD43^{low}$ cells that generated T cells. These hESC-derived T cells proliferated in response to

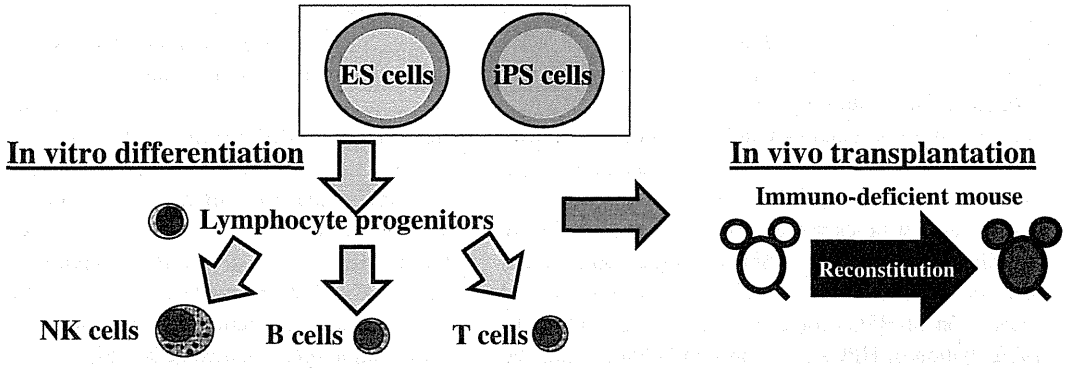

Cell types	Surface markers		Specific genes		Other characteristics
	Mouse	Human	Mouse	Human	
T cells	CD4, 8 TCR	TCR, CD3 CD4, CD7, CD8, CD45	*Rag1* *Hes1* *Gata3*	*HES1* *CD3* *GATA3*	1) Cytokine production 2) T cell differentiation in transplanted mouse (In vivo)
B cells	B220 CD19	CD10 CD19 CD45	*IgM* *Pax5*	*IgM* *PAX5* *λ-like*	1) Rearrangement of VDJ 2) Rearrangement of VJ
NK cells	CD94	CD45 CD56 CD94	*CD94, Ly49, NKR-P1, Granzyme A,B*	*CD122* *ID2* *ID3*	1) Cytotoxity 2) Cytokine production

Fig. 6 Schematic diagram of pluripotent cell-derived lymphocytes. ES and iPS cells-derived T cells are characterized by the expression of surface markers (CD4, CD8 and T cell receptor (TCR) in mouse; TCR, CD3, CD4, CD7, CD8 and CD45 in human) and specific transcription factor genes (*Rag1, Hes1* and *Gata3* in mouse; *HES1, CD3* and *GATA3* in human). A representative characteristic of T cells is cytokine (interleukin-2 and interferon-γ) production in response to anti-CD3 antibody and PMA in vitro. To further investigate the in vivo differentiation of pluripotent cells into T cells, pluripotent cells are transplanted into congenic mice in the mouse T cells and SCID-hu mice in human, respectively. ES and iPS cells-derived B cells are characterized by the expression of surface markers (B220 and CD19 in mouse; CD10, CD19 and CD45 in human) and specific transcription factor genes (*IgM* and *PAX5* in both mouse and human). A representative characteristic of B cells is VDJ and VJ gene rearrangement, which reveals early B cell commitment from pro-B cell to pre-B cells, and from pre-B cells to immature-B cells, respectively. Other characteristic of B cells is the protein expression of immunoglobulin chains such as μH chain composing pre-B receptor and L-chain for IgM, respectively. ES and iPS cells-derived NK cells are characterized by the expression of surface markers (CD94 in mouse; CD45, CD56 and CD94 in human) and specific transcription factor genes (*CD94, Ly49, NKR-P1, Granzyme A* and *Granzyme B* in mouse; *CD122, Inhibitor of DNA binding (ID) 2* and *ID3* in human). The representative characteristics of NK cells are tested by cytotoxity assay and cytokine (interleukine-6 and tumor necrosis factor alpha) production in vitro, which reveals the abilities to kill the tumor cells and to initiate the immune reaction, respectively

PHA stimulation, suggesting that hESCs can give rise to functional T cells [63]. Nevertheless, $CD34^+CD45^+$ cells from hESCs did not produce T cells on either OP9-DL1 monolayers or in FTOC cultures [64].

Mouse ES cells co-cultured with OP9 cells in the presence of Flt3-L, IL-15, IL-6, IL-7 and SCF generated NK cells, which were positive for CD94/NKG2 receptors and functioned to kill certain tumor lines and MHC class-I-deficient lymphoblasts [65]. Natural killer T (NKT) cells are a heterogeneous group of T cells that share properties of both T and NK cells. The OP9-DL1 method was also useful for NKT cell differentiation of mouse iPS cells established from MEFs and adult splenic NKT cells. iPS-derived NKT cells secreted the Th1 cytokine IFN-γ in response to in vitro stimulation and could recapitulate the adjuvant effect and suppress tumor growth in vivo [66].

Ni et al. reported NK cell generation from human H9 ES and BJ1-iPS12 iPS cells established from healthy adult human dermal fibroblasts. Among $CD45^+CD56^+$ cells generated, $CD117^-CD94^+$cells were mature NK cells with cytotoxic activity in vitro. In addition, both ES cell- and iPS cell-derived NK cells inhibited HIV-1 infection of a CEM cell line and of human primary $CD4^+$ T cells via killing through direct lysis, antibody-dependent cellular cytotoxicity, and production of chemokines and cytokines [67].

Perspective

Basic researchers have established methods for HSC and mature HC differentiation from ES and iPS cells that could

be useful for potential transplantation and transfusion therapy. Time will be required to standardize these methods, since individual researchers use diverse materials and methods, resulting in varied differentiation capability among ES and iPS cells, depending on cell line, passage number, methylation status and cell origin. To minimize clinical risks, special attention to potential tumorigenicity of manipulated cells must be paid. Although culture conditions, such as use of feeder-free cultures or serum-free media have already been improved, it remains necessary to shorten culture periods for iPS cell establishment and differentiation of the desired cell lineage induction from ES or iPS cells. Recently, "direct conversion" from human fibroblasts to HPCs and mature HCs was reported without establishing iPS cells [68]. In that case, ectopic expression of OCT4 plus treatment with a specific cytokine was effective to induce the $CD45^{+}$ cells, which had in vivo engraftment capacity. This method represents a new approach for autologous cell-transplant therapies that avoids difficulties involved with using human pluripotent stem cells. Thus, some issues remain to be resolved before ES and iPS cells can be applied to regenerative medicine.

Acknowledgments We thank Dr. Koichi Akashi, Dr. Kasem Kulkeaw, Ms. Yuka Horio, Ms. Chiyo Mizuochi, Ms. WaiFeng Lim and Dr. Elise Larmar for research support, and grant supports from the Ministry of Education, Culture, Sports, Science and Technology, the Ministry of Health, Labor and Welfare, and the Japan Society for the Promotion of Science.

Conflict of interest The authors indicate no potential conflicts of interest.

References

1. Dzierzak, E., & Speck, N. A. (2008). Of lineage and legacy: the development of mammalian hematopoietic stem cells. *Nature Immunology, 9*, 129–136.
2. Wang, L. D., & Wagers, A. J. (2011). Dynamic niches in the origination and differentiation of haematopoietic stem cells. *Nature Reviews Molecular Cell Biology, 12*, 643–655.
3. Mizuochi, C., Fraser, S. T., Biasch, K., Horio, Y., Kikushige, Y., Tani, K., Akashi, K., Tavian, M., & Sugiyama, D. (2012). Intra-aortic clusters undergo endothelial to hematopoietic phenotypic transition during early embryogenesis. *PLoS One*; in press.
4. Sasaki, T., Mizuochi, C., Horio, Y., Nakao, K., Akashi, K., & Sugiyama, D. (2010). Regulation of hematopoietic cell clusters in the placental niche through SCF/Kit signaling in embryonic mouse. *Development, 137*, 3941–3952.
5. Sugiyama, D., Kulkeaw, K., Mizuochi, C., Horio, Y., & Okayama, S. (2011). Hepatoblasts comprise a niche for fetal liver erythropoiesis through cytokine production. *Biochemical and Biophysical Research Communications, 410*, 301–306.
6. Sugiyama, D., Inoue-Yokoo, T., Fraser, S. T., Kulkeaw, K., Mizuochi, C., & Horio, Y. (2011). Embryonic regulation of the mouse hematopoietic niche. *Scientific World Journal, 11*, 1770–1780.
7. Evans, M. J., & Kaufman, M. H. (1981). Establishment in culture of pluripotential cells from mouse embryos. *Nature, 292*, 154–156.
8. Takahashi, K., & Yamanaka, S. (2006). Induction of pluripotent stem cells from mouse embryonic and adult fibroblast cultures by defined factors. *Cell, 126*, 663–676.
9. Orr-Urtreger, A., Bedford, M. T., Do, M. S., Eisenbach, L., & Lonai, P. (1992). Developmental expression of the alpha receptor for platelet-derived growth factor, which is deleted in the embryonic lethal Patch mutation. *Development, 115*, 289–303.
10. Takakura, N., Yoshida, H., Ogura, Y., Kataoka, H., & Nishikawa, S. (1997). PDGFR alpha expression during mouse embryogenesis: immunolocalization analyzed by whole-mount immunohistostaining using the monoclonal anti-mouse PDGFR alpha antibody APA5. *Journal of Histochemistry and Cytochemistry, 45*, 883–893.
11. Kabrun, N., Buhring, H. J., Choi, K., Ullrich, A., Risau, W., & Keller, G. (1997). Flk-1 expression defines a population of early embryonic hematopoietic precursors. *Development, 124*, 2039–2048.
12. Choi, K., Kennedy, M., Kazarov, A., Papadimitriou, J. C., & Keller, G. (1998). A common precursor for hematopoietic and endothelial cells. *Development, 125*, 725–732.
13. Fehling, H. J., Lacaud, G., Kubo, A., et al. (2003). Tracking mesoderm induction and its specification to the hemangioblast during embryonic stem cell differentiation. *Development, 130*, 4217–4227.
14. Sakurai, H., Era, T., Jakt, L. M., Okada, M., Nakai, S., & Nishikawa, S. (2006). In vitro modeling of paraxial and lateral mesoderm differentiation reveals early reversibility. *Stem Cells, 24*, 575–586.
15. Kulkeaw, K., Horio, Y., Mizuochi, C., Ogawa, M., & Sugiyama, D. (2010). Variation in hematopoietic potential of induced pluripotent stem cell lines. *Stem Cell Reviews, 6*, 381–389.
16. Inoue, T., Kulkeaw, K., Okayama, S., Tani, K., & Sugiyama, D. (2011). Variation in mesodermal and hematopoietic potential of adult skin-derived induced pluripotent stem cell lines in mice. *Stem Cell Reviews, 7*, 958–968.
17. Niwa, A., Heike, T., Umeda, K., et al. (2011). A novel serum-free monolayer culture for orderly hematopoietic differentiation of human pluripotent cells via mesodermal progenitors. *PLoS One, 6*, e22261.
18. Morishima, T., Watanabe, K., Niwa, A., et al. (2011). Neutrophil differentiation from human-induced pluripotent stem cells. *Journal of Cellular Physiology, 226*, 1283–1291.
19. Grigoriadis, A. E., Kennedy, M., Bozec, A., et al. (2010). Directed differentiation of hematopoietic precursors and functional osteoclasts from human ES and iPS cells. *Blood, 115*, 2769–2776.
20. Tolar, J., Park, I. H., Xia, L., et al. (2011). Hematopoietic differentiation of induced pluripotent stem cells from patients with mucopolysaccharidosis type I (Hurler syndrome). *Blood, 117*, 839–847.
21. Burt, R. K., Verda, L., Kim, D. A., Oyama, Y., Luo, K., & Link, C. (2004). Embryonic stem cells as an alternate marrow donor source: engraftment without graft-versus-host disease. *The Journal of Experimental Medicine, 199*, 895–904.
22. Kyba, M., Perlingeiro, R. C., & Daley, G. Q. (2002). HoxB4 confers definitive lymphoid-myeloid engraftment potential on embryonic stem cell and yolk sac hematopoietic progenitors. *Cell, 109*, 29–37.
23. Wang, Y., Yates, F., Naveiras, O., Ernst, P., & Daley, G. Q. (2005). Embryonic stem cell-derived hematopoietic stem cells. *Proceedings of the National Academy of Sciences of the United States of America, 102*, 19081–19086.
24. Zhang, X. B., Beard, B. C., Trobridge, G. D., et al. (2008). High incidence of leukemia in large animals after stem cell gene therapy with a HOXB4-expressing retroviral vector. *The Journal of Clinical Investigation, 118*, 1502–1510.
25. Hanna, J., Wernig, M., Markoulaki, S., et al. (2007). Treatment of sickle cell anemia mouse model with iPS cells generated from autologous skin. *Science, 318*, 1920–1923.
26. Lin, J., Fernandez, I., & Roy, K. (2011). Development of feeder-free culture systems for generation of ckit+sca1+ progenitors from mouse iPS cells. *Stem Cell Reviews, 7*, 736–747.
27. Wang, L., Menendez, P., Shojaei, F., et al. (2005). Generation of hematopoietic repopulating cells from human embryonic stem

cells independent of ectopic HOXB4 expression. *The Journal of Experimental Medicine, 201*, 1603–1614.
28. Nakano, T., Kodama, H., & Honjo, T. (1994). Generation of lymphohematopoietic cells from embryonic stem cells in culture. *Science, 265*, 1098–1101.
29. Nakano, T., Kodama, H., & Honjo, T. (1996). In vitro development of primitive and definitive erythrocytes from different precursors. *Science, 272*, 722–724.
30. Motoyama, N., Kimura, T., Takahashi, T., Watanabe, T., & Nakano, T. (1999). bcl-x prevents apoptotic cell death of both primitive and definitive erythrocytes at the end of maturation. *The Journal of Experimental Medicine, 189*, 1691–1698.
31. Keller, G., Kennedy, M., Papayannopoulou, T., & Wiles, M. V. (1993). Hematopoietic commitment during embryonic stem cell differentiation in culture. *Molecular and Cellular Biology, 13*, 473–486.
32. Carotta, S., Pilat, S., Mairhofer, A., et al. (2004). Directed differentiation and mass cultivation of pure erythroid progenitors from mouse embryonic stem cells. *Blood, 104*, 1873–1880.
33. Ma, F., Ebihara, Y., Umeda, K., et al. (2008). Generation of functional erythrocytes from human embryonic stem cell-derived definitive hematopoiesis. *Proceedings of the National Academy of Sciences of the United States of America, 105*, 13087–13092.
34. Lu, S. J., Feng, Q., Park, J. S., et al. (2008). Biologic properties and enucleation of red blood cells from human embryonic stem cells. *Blood, 112*, 4475–4484.
35. Lengerke, C., Grauer, M., Niebuhr, N. I., et al. (2009). Hematopoietic development from human induced pluripotent stem cells. *Annals of the New York Academy of Sciences, 1176*, 219–227.
36. Raya, A., Rodriguez-Piza, I., Guenechea, G., et al. (2009). Disease-corrected haematopoietic progenitors from Fanconi anaemia induced pluripotent stem cells. *Nature, 460*, 53–59.
37. Ye, Z., Zhan, H., Mali, P., et al. (2009). Human-induced pluripotent stem cells from blood cells of healthy donors and patients with acquired blood disorders. *Blood, 114*, 5473–5480.
38. Era, T., Takagi, T., Takahashi, T., Bories, J. C., & Nakano, T. (2000). Characterization of hematopoietic lineage-specific gene expression by ES cell in vitro differentiation induction system. *Blood, 95*, 870–878.
39. Eto, K., Murphy, R., Kerrigan, S. W., et al. (2002). Megakaryocytes derived from embryonic stem cells implicate CalDAG-GEFI in integrin signaling. *Proceedings of the National Academy of Sciences of the United States of America, 99*, 12819–12824.
40. Fujimoto, T. T., Kohata, S., Suzuki, H., Miyazaki, H., & Fujimura, K. (2003). Production of functional platelets by differentiated embryonic stem (ES) cells in vitro. *Blood, 102*, 4044–4051.
41. Kaufman, D. S., Hanson, E. T., Lewis, R. L., Auerbach, R., & Thomson, J. A. (2001). Hematopoietic colony-forming cells derived from human embryonic stem cells. *Proceedings of the National Academy of Sciences of the United States of America, 98*, 10716–10721.
42. Gaur, M., Kamata, T., Wang, S., Moran, B., Shattil, S. J., & Leavitt, A. D. (2006). Megakaryocytes derived from human embryonic stem cells: a genetically tractable system to study megakaryocytopoiesis and integrin function. *Journal of Thrombosis and Haemostasis, 4*, 436–442.
43. Takayama, N., Nishikii, H., Usui, J., et al. (2008). Generation of functional platelets from human embryonic stem cells in vitro via ES-sacs, VEGF-promoted structures that concentrate hematopoietic progenitors. *Blood, 111*, 5298–5306.
44. Takayama, N., Nishimura, S., Nakamura, S., et al. (2010). Transient activation of c-MYC expression is critical for efficient platelet generation from human induced pluripotent stem cells. *The Journal of Experimental Medicine, 207*, 2817–2830.
45. Wiles, M. V., & Keller, G. (1991). Multiple hematopoietic lineages develop from embryonic stem (ES) cells in culture. *Development, 111*, 259–267.
46. Lindmark, H., Rosengren, B., Hurt-Camejo, E., & Bruder, C. E. (2004). Gene expression profiling shows that macrophages derived from mouse embryonic stem cells is an improved in vitro model for studies of vascular disease. *Experimental Cell Research, 300*, 335–344.
47. Moore, K. J., Fabunmi, R. P., Andersson, L. P., & Freeman, M. W. (1998). In vitro-differentiated embryonic stem cell macrophages: a model system for studying atherosclerosis-associated macrophage functions. *Arteriosclerosis, Thrombosis, and Vascular Biology, 18*, 1647–1654.
48. Senju, S., Haruta, M., Matsunaga, Y., et al. (2009). Characterization of dendritic cells and macrophages generated by directed differentiation from mouse induced pluripotent stem cells. *Stem Cells, 27*, 1021–1031.
49. Lieber, J. G., Webb, S., Suratt, B. T., et al. (2004). The in vitro production and characterization of neutrophils from embryonic stem cells. *Blood, 103*, 852–859.
50. Yokoyama, Y., Suzuki, T., Sakata-Yanagimoto, M., et al. (2009). Derivation of functional mature neutrophils from human embryonic stem cells. *Blood, 113*, 6584–6592.
51. Saeki, K., Nakahara, M., Matsuyama, S., et al. (2009). A feeder-free and efficient production of functional neutrophils from human embryonic stem cells. *Stem Cells, 27*, 59–67.
52. Choi, K. D., Vodyanik, M. A., & Slukvin, I. I. (2009). Generation of mature human myelomonocytic cells through expansion and differentiation of pluripotent stem cell-derived lin-CD34+CD43+CD45+ progenitors. *The Journal of Clinical Investigation, 119*, 2818–2829.
53. Zou, J., Sweeney, C. L., Chou, B. K., et al. (2011). Oxidase-deficient neutrophils from X-linked chronic granulomatous disease iPS cells: functional correction by zinc finger nuclease-mediated safe harbor targeting. *Blood, 117*, 5561–5572.
54. Cho, S. K., Webber, T. D., Carlyle, J. R., Nakano, T., Lewis, S. M., & Zuniga-Pflucker, J. C. (1999). Functional characterization of B lymphocytes generated in vitro from embryonic stem cells. *Proceedings of the National Academy of Sciences of the United States of America, 96*, 9797–9802.
55. Wada, H., Kojo, S., Kusama, C., et al. (2011). Successful differentiation to T cells, but unsuccessful B-cell generation, from B-cell-derived induced pluripotent stem cells. *International Immunology, 23*, 65–74.
56. Vodyanik, M. A., Bork, J. A., Thomson, J. A., & Slukvin, I. I. (2005). Human embryonic stem cell-derived CD34+ cells: efficient production in the coculture with OP9 stromal cells and analysis of lymphohematopoietic potential. *Blood, 105*, 617–626.
57. Carpenter, L., Malladi, R., Yang, C. T., et al. (2011). Human induced pluripotent stem cells are capable of B-cell lymphopoiesis. *Blood, 117, 4008–4011.*
58. de Pooter, R. F., Cho, S. K., Carlyle, J. R., & Zuniga-Pflucker, J. C. (2003). In vitro generation of T lymphocytes from embryonic stem cell-derived prehematopoietic progenitors. *Blood, 102*, 1649–1653.
59. Schmitt, T. M., de Pooter, R. F., Gronski, M. A., Cho, S. K., Ohashi, P. S., & Zuniga-Pflucker, J. C. (2004). Induction of T cell development and establishment of T cell competence from embryonic stem cells differentiated in vitro. *Nature Immunology, 5*, 410–417.
60. Lei, F., Haque, R., Weiler, L., Vrana, K. E., & Song, J. (2009). T lineage differentiation from induced pluripotent stem cells. *Cellular Immunology, 260*, 1–5.
61. Galic, Z., Kitchen, S. G., Kacena, A., et al. (2006). T lineage differentiation from human embryonic stem cells. *Proceedings of the National Academy of Sciences of the United States of America, 103*, 11742–11747.
62. Galic, Z., Kitchen, S. G., Subramanian, A., et al. (2009). Generation of T lineage cells from human embryonic stem cells in a feeder free system. *Stem Cells, 27*, 100–107.
63. Timmermans, F., Velghe, I., Vanwalleghem, L., et al. (2009). Generation of T cells from human embryonic stem cell-derived hematopoietic zones. *Journal of Immunology, 182*, 6879–6888.
64. Martin, C. H., Woll, P. S., Ni, Z., Zuniga-Pflucker, J. C., & Kaufman, D. S. (2008). Differences in lymphocyte developmental potential

between human embryonic stem cell and umbilical cord blood-derived hematopoietic progenitor cells. *Blood, 112*, 2730–2737.
65. Lian, R. H., Maeda, M., Lohwasser, S., et al. (2002). Orderly and nonstochastic acquisition of CD94/NKG2 receptors by developing NK cells derived from embryonic stem cells in vitro. *Journal of Immunology, 168*, 4980–4987.
66. Watarai, H., Fujii, S., Yamada, D., et al. (2010). Murine induced pluripotent stem cells can be derived from and differentiate into natural killer T cells. *The Journal of Clinical Investigation, 120*, 2610–2618.
67. Ni, Z., Knorr, D. A., Clouser, C. L., et al. (2011). Human pluripotent stem cells produce natural killer cells that mediate anti-HIV-1 activity by utilizing diverse cellular mechanisms. *Journal of Virology, 85*, 43–50.
68. Szabo, E., Rampalli, S., Risueno, R. M., et al. (2010). Direct conversion of human fibroblasts to multilineage blood progenitors. *Nature, 468, 521–526.*

OPEN ACCESS Freely available online

PLoS one

Intra-Aortic Clusters Undergo Endothelial to Hematopoietic Phenotypic Transition during Early Embryogenesis

Chiyo Mizuochi[1], Stuart T. Fraser[2], Katia Biasch[3], Yuka Horio[1], Yoshikane Kikushige[4], Kenzaburo Tani[5], Koichi Akashi[4], Manuela Tavian[3], Daisuke Sugiyama[1]*

1 Department of Hematopoietic Stem Cells,SSP Stem Cell Unit, Kyushu University Faculty of Medical Sciences, Fukuoka, Japan, **2** Laboratory of Blood Cell Development, Disciplines of Physiology, Anatomy and Histology, School of Medical Sciences, University of Sydney, Camperdown, New South Wales, Australia, **3** Unité 682 INSERM, Strasbourg, France, **4** Department of Medicine and Biosystemic Science, Kyushu University Graduate School of Medical Sciences, Fukuoka, Japan, **5** Department of Molecular Genetics, Medical Institute of Bioregulation, Kyushu University, Fukuoka, Japan

Abstract

Intra-aortic clusters (IACs) attach to floor of large arteries and are considered to have recently acquired hematopoietic stem cell (HSC)-potential in vertebrate early mid-gestation embryos. The formation and function of IACs is poorly understood. To address this issue, IACs were characterized by immunohistochemistry and flow cytometry in mouse embryos. Immunohistochemical analysis revealed that IACs simultaneously express the surface antigens CD31, CD34 and c-Kit. As embryos developed from 9.5 to 10.5 dpc, IACs up-regulate the hematopoietic markers CD41 and CD45 while down-regulating the endothelial surface antigen VE-cadherin/CD144, suggesting that IACs lose endothelial phenotype after 9.5 dpc. Analysis of the hematopoietic potential of IACs revealed a significant change in macrophage CFC activity from 9.5 to 10.5 dpc. To further characterize IACs, we isolated IACs based on CD45 expression. Correspondingly, the expression of hematopoietic transcription factors in the CD45(neg) fraction of IACs was significantly up-regulated. These results suggest that the transition from endothelial to hematopoietic phenotype of IACs occurs after 9.5 dpc.

Citation: Mizuochi C, Fraser ST, Biasch K, Horio Y, Kikushige Y, et al. (2012) Intra-Aortic Clusters Undergo Endothelial to Hematopoietic Phenotypic Transition during Early Embryogenesis. PLoS ONE 7(4): e35763. doi:10.1371/journal.pone.0035763

Editor: Alfons Navarro, University of Barcelona, Spain

Received March 3, 2011; **Accepted** March 22, 2012; **Published** April 27, 2012

Funding: This research was supported in part by the Project for Realization of Regenerative Medicine, Special Coordination Funds for Promoting Science and Technology of the Ministry of Education, Science, Sports and Culture (www.mext.go.jp/english); and SAKURA program of the Japan Society for the Promotion of Science (www.jsps.go.jp/english/index.html). The funders had no role in study design, data collection and analysis, decision to publish, or preparation of the manuscript.

Competing Interests: The authors have declared that no competing interests exist.

* E-mail: ds-mons@yb3.so-net.ne.jp

Introduction

During mouse embryogenesis, hematopoiesis begins at the extra-embryonic yolk sac (YS) at 7.5 days post-coitum (dpc) and shifts to fetal liver after mid-gestation, then to spleen and finally to bone marrow shortly before birth. There are two distinct waves of hematopoietic emergence: a transient wave, primarily restricted to erythropoiesis in YS blood islands prior to the connection of the circulation from the YS to the embryo; and a definitive wave originating in both the YS and embryo proper. The embryonic site has been identified in the aortic region, in the para-aortic splanchnopleura (p-Sp)/aorta-gonad-mesonephros (AGM) region [1–6]. Functional hematopoietic stem cells (HSCs) that can reconstitute adult recipients are first identified in the AGM region at 10.5 dpc after ex vivo organ culture [7]. The cells at 10.5 dpc that were not cultured ex vivo rarely reconstitute adult recipients, whereas those at 11.5 dpc can regardless [7–9]. Therefore, the cells that acquire HSC activity after culture step, have been termed "pre-HSC"s. Although several reports characterize the surface marker expression on both pre-HSCs at 10.5 dpc and HSCs at 11.5 dpc, the developmental process of HSC generation still remains unclear [8–11]. Cell populations capable of reconstituting neonatal recipients are detected in the p-Sp/AGM region at 9.5 dpc [12–13]. These observations suggest that ancestor cells of HSC from the p-Sp/AGM region at 9.5 dpc require special microenvironments to acquire HSC activity and that HSCs undergo phenotypic changes from 9.5 to 10.5 dpc. In the AGM region, intra-aortic/arterial clusters (IACs) are observed attached to floors of large arteries in several species including chicken, mouse and humans [3]. Mouse IACs have been characterized morphologically and are primarily located in three large arteries, namely, the dorsal aorta (DA), the omphalomesenteric (vitelline) artery (OMA; VA) and the umbilical artery (UA) [3,14–15]. IACs express both hematopoietic (CD41 and CD45) and endothelial (CD31, CD34 and VE-cadherin) surface markers [3,15–16] suggesting that IACs are likely equivalent to ancestor cells of HSC and/or pre-HSCs and are derived from endothelial cells (ECs) at aortic/arterial regions. Although recent genetic approaches and novel tracing methods demonstrate that IACs are derived from ECs in zebrafish and mice, it is unclear how IACs form and acquire HSC activity [17–25].

To address how IACs form and function in HSC generation, we first visualized IACs by immunohistochemistry and confocal imaging and were found to simultaneously express CD31, CD34 and c-Kit. This approach enabled us to investigate the phenotypic

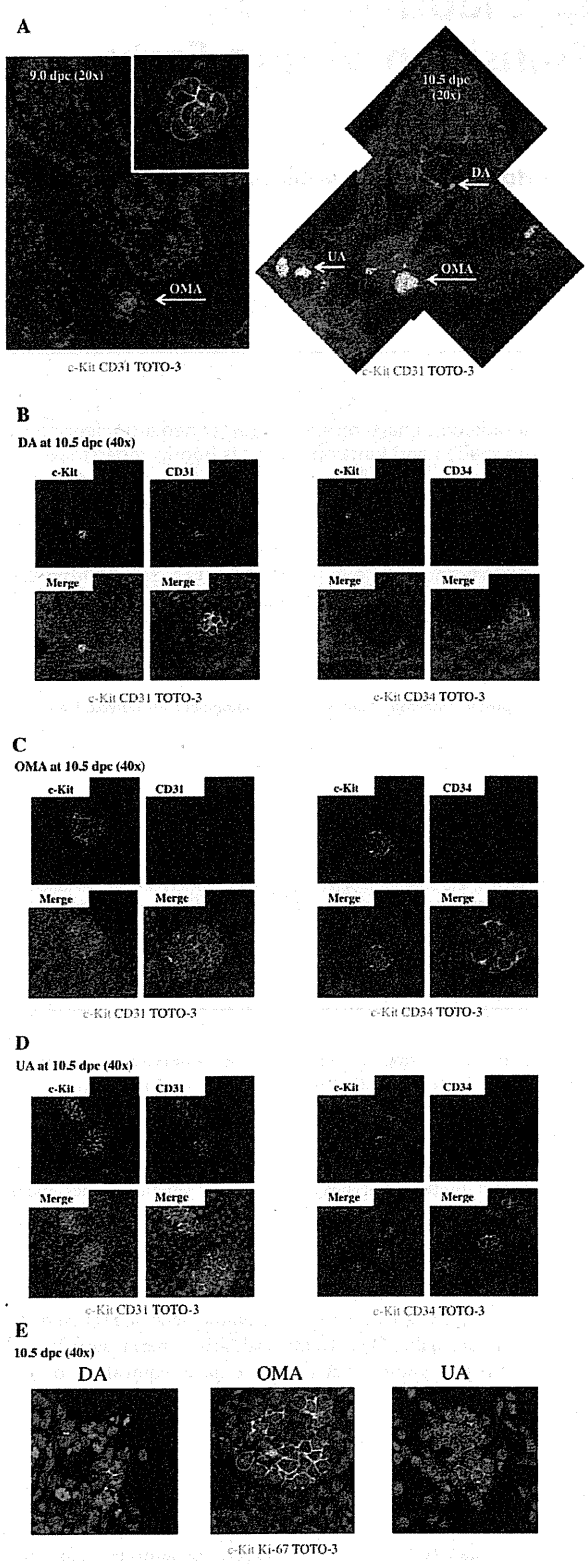

Figure 1. Confocal images of IACs expressing CD31/CD34/c-Kit in the AGM region. Transverse sections of AGM region from ICR mouse embryos at 9.0 and 10.5 dpc were stained with antibodies and observed by confocal microscopy. (**A**) IACs were observed in the omphalomesenteric artery (OMA) at 9.0 dpc (left; magnified view of IACs in upper right panel) and in the OMA, dorsal aorta (DA) and umbilical artery (UA) at 10.5 dpc (right). CD31 (red), c-Kit (green), and TOTO-3 (blue). Arrows indicate IACs. Original magnification is 20x. (**B-D**) IACs were observed in the DA (B), OMA (C) and UA (D) at 10.5 dpc. Left panel shows staining for CD31 (red), c-Kit (green), and TOTO-3 (blue), and right panel shows staining for CD34 (red), c-Kit (green), and TOTO-3 (blue) staining. Images were taken at 40x and zoom was used to show a detail at right lower panel. Another IAC in the DA is shown in Figure S1. (**E**) IACs expressing Ki-67, a marker of proliferation, were observed in the DA (left), OMA (middle) and UA (right). Ki-67 (red), c-Kit (green), and TOTO-3 (blue). Images were taken at 40x and zoom was used to show a detail.
doi:10.1371/journal.pone.0035763.g001

characterization of IACs by flow cytometry and hematopoiesis assays. Here, we demonstrate a significant transition from endothelial to hematopoietic cell phenotype of IAC cells after 9.5 dpc.

Results

Visualization of IACs in mouse embryos

Previous studies identified intra-aortic/arterial clusters (IACs) primarily by immunocytochemistry and microscopy [3,14–15]. Recently, we successfully visualized hematopoietic cell clusters in mouse placenta using thick (20 μm) cryo-sections and antibodies recognizing the embryonic HSC markers c-Kit, CD31 and CD34 and applied this method to quantifying IACs [26]. Cell aggregates consisting of more than three c-Kit-positive cells were defined as an IAC. Here, we used confocal microscopy to expand upon our previous study and characterize the cell types found within IACs according to c-Kit, CD31 and CD34 expression (Figure 1). The first IACs were observed as spherical structures in the omphalomesentric artery (OMA) at 9.0 dpc (12–14 somite pairs [SP]) (Figure 1A, left). Between 9.5 dpc (18–22 SP) to 10.5 dpc (30–34 SP), large arteries such as the dorsal aorta (DA), OMA and umbilical artery (UA) form [14]. IACs were observed in DA, OMA and UA at 10.5 dpc, and the size of IACs in the OMA and UA was significantly larger than those seen in the DA (Figure 1A, right). Localization of IACs in DA was not restricted to the ventral wall of DA, but rather some IACs were observed at dorsal and lateral sides of the wall (data not shown). All IACs in the DA, OMA and UA at 10.5 dpc simultaneously expressed c-Kit, CD31 and CD34 (Figure 1B-D). IACs expressing c-Kit in the different arteries analyzed were also positive for Ki-67, a marker of cell proliferation, regardless of location, suggesting that cells within IACs are highly proliferative (Figure 1E).

Characterization of IACs by flow cytometry and hematopoietic progenitor assays

To further characterize IACs, the caudal portion of embryos containing the p-Sp/AGM region was dissociated and analyzed by flow cytometry. At 10.5 dpc, c-Kit$^+$/CD31$^+$/CD34$^+$ cells, which are equivalent to IACs, were assessed for expression of the cell surface markers VE-cadherin/CD144 (an endothelial cell marker), CD41 (the earliest hematopoietic cell marker), CD45 (a pan-leukocyte marker), Sca-1 (a late fetal and adult HSC marker) and CD150 and EPCR (adult HSC markers) (Figure 2A-H). c-Kit$^+$/CD31$^+$/CD34$^+$ cells represented 0.069±0.01% in whole caudal portion of embryos. Among c-Kit$^+$/CD31$^+$/CD34$^+$ cells, VE-cadherin surface antigen expression decreased significantly within 24 hours from 9.5 to 10.5 dpc. Concomitantly, expression of the hematopoietic markers CD41 and CD45 increased from negative or low levels of expression on IAC cells at 9.5 dpc to abundant

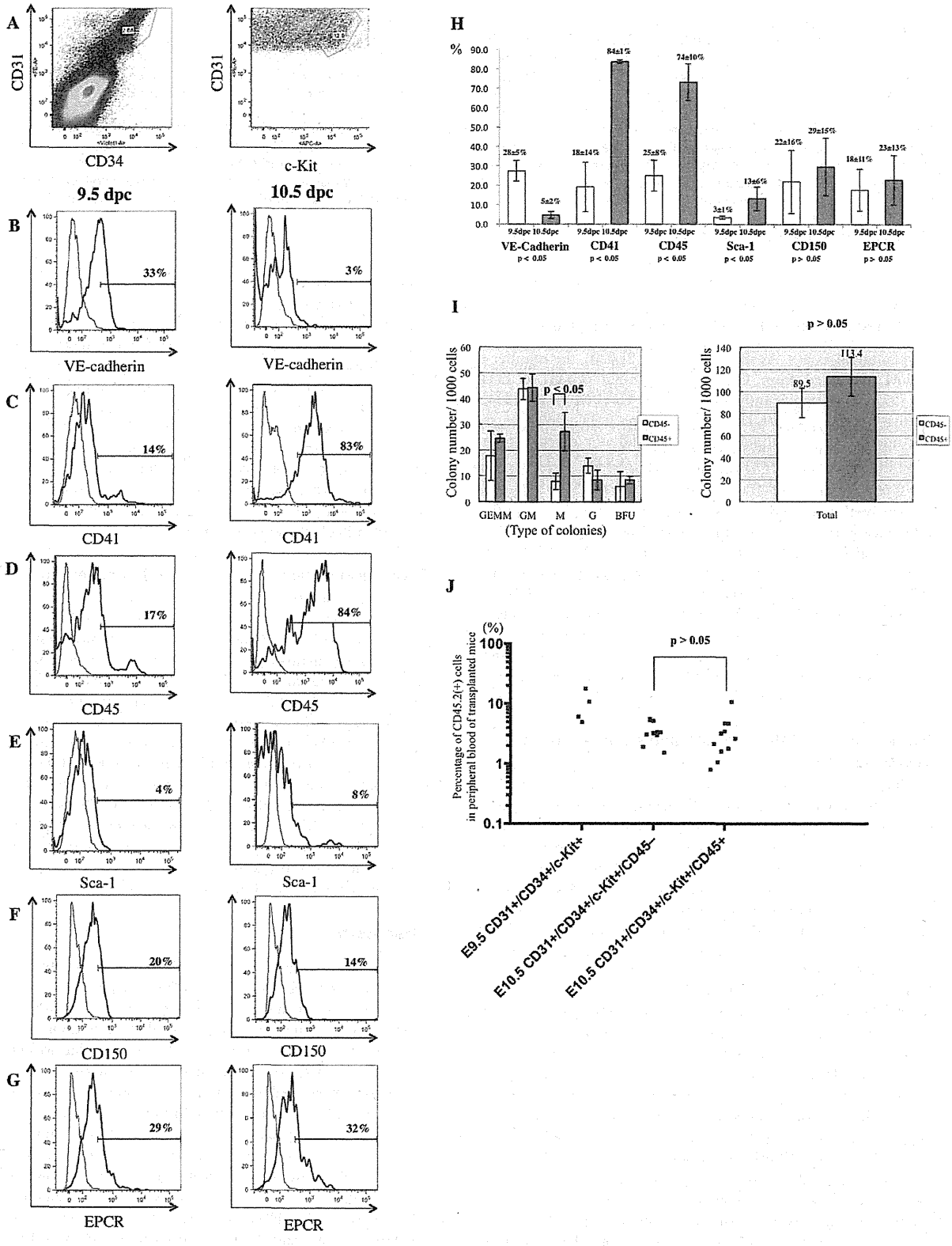

Figure 2. Flow cytometric analysis of CD31$^+$/CD34$^+$/c-Kit$^+$ AGM cells using surface expression of hematopoietic and endothelial cell markers. Single cell suspensions of the caudal portion of embryos containing the p-Sp/AGM region at 9.5 and 10.5 dpc were prepared and analyzed by flow cytometry. (**A**) Cells expressing CD31, CD34 and c-Kit markers of IACs were gated first. Isotype control of flow cytometric analysis is shown in

Figure S2. (**B-G**) Expression of hematopoietic and endothelial cell markers was analyzed on CD31$^+$/CD34$^+$/c-Kit$^+$ cells at 9.5 dpc (left) and 10.5 dpc (right) with the following antibodies: (**B**) VE-cadherin/CD144 (an endothelial cell marker), (**C**) CD41 (the earliest hematopoietic cell marker), (**D**) CD45 (a pan-leukocyte marker), (**E**) Sca-1 (a late fetal and adult HSC marker), (**F**) CD150 and (**G**) EPCR (adult HSC markers). At least 1,000 cells were assessed for each surface antigen. Representative profiles are shown. (**H**) Percentage of expression was summarized. At least 3 independent experiments were performed. Mean ± 2SD was calculated and shown at the top of bars. (**I**) One thousand sorted CD45-negative or CD45-positive CD31$^+$/CD34$^+$/c-Kit$^+$ cells were cultured in semisolid medium containing the hematopoietic cytokines, SCF (Stem Cell Factor), IL (Interleukin)-3, IL-6 and EPO (Erythropoietin). Left and right panels show each fraction and the total number of colonies, respectively. GEMM (colony-forming units of granulocyte erythrocyte monocyte macrophages); GM (of granulocyte macrophages); M (of macrophages); G (of granulocytes); BFU (burst forming units of erythroid cells). (**J**) 50–100 sorted CD31$^+$/CD34$^+$/c-Kit$^+$ cells at 9.5 dpc, as well as CD45-negative and CD45-positive CD31$^+$/CD34$^+$/c-Kit$^+$ cells were transplanted into busulfan-treated Ly5.1 mouse neonates. Approximately one year after transplantation, blood samples were collected and analyzed for CD45.2 expression by flow cytometry. Representative profile of flow cytometric analysis and its negative and positive controls are shown in Figure S3 and S6, respectively.
doi:10.1371/journal.pone.0035763.g002

levels at 10.5 dpc. Sca-1 expression also increased from 9.5 to 10.5 dpc.

We next separated c-Kit$^+$/CD31$^+$/CD34$^+$ cells based on CD45 expression by flow cytometry and performed colony assays and transplantation assays. As shown in Figure 2I (left), the number of CFU-M generated from CD45-positive c-Kit$^+$/CD31$^+$/CD34$^+$ cells (27.3) was significantly higher than CFU-M from CD45-negative c-Kit$^+$/CD31$^+$/CD34$^+$ cells (8.0) ($p<0.05$). However, the total number of hematopoietic colonies did not differ between CD45-negative and CD45-positive c-Kit$^+$/CD31$^+$/CD34$^+$ cells ($p>0.05$). When 50–100 c-Kit$^+$/CD31$^+$/CD34$^+$ cells were transplanted into neonate recipients, there was no significant difference in reconstitution ability (CD45-negative, 3.55%; CD45-positive 3.07%) ($p>0.05$) (Figure 2J). c-Kit$^+$/CD31$^+$/CD34$^+$ cells at 9.5 dpc were able to reconstitute recipients and chimerism to 9.89% was achieved. Presumptive ancestor cells of HSC can reportedly reconstitute neonate recipients but not adult recipients [13]. In addition, pre-HSCs at 10.5 dpc rarely reconstitute adult recipients without culture step [7–9,11]. When 100 c-Kit$^+$/CD31$^+$/CD34$^+$ cells were transplanted into adult recipients, no reconstitution was observed (data not shown).

Expression of CD45 in mouse and human intra-aortic/arterial clusters

CD45-negative and CD45-positive c-Kit$^+$/CD31$^+$/CD34$^+$ cells showed no difference in hematopoietic potential except within the macrophage lineage. To further investigate a role of CD45 expression on c-Kit$^+$/CD31$^+$/CD34$^+$ cells, we used flow cytometry to segregate c-Kit$^+$/CD31$^+$/CD34$^+$ cells into three fractions. Three distinct populations became apparent; CD45negative cells, CD45low cells, and CD45high cells (Figure 3A). The proportion of CD45-negative and CD45-low positive c-Kit$^+$/CD31$^+$/CD34$^+$ cells was higher at 9.5 dpc than at 10.5 dpc, whereas the percentage of CD45-high positive c-Kit$^+$/CD31$^+$/CD34$^+$ cells increased by 5-fold at 10.5 dpc (31.0%) compared to 9.5 dpc (6.3%) (Figure 3B). These data suggest that CD45-negative c-Kit$^+$/CD31$^+$/CD34$^+$ cells are precursors of CD45-high positive c-Kit$^+$/CD31$^+$/CD34$^+$ cells and that CD45 is a marker of IAC maturation. To address this issue, we examined expression levels of the gene encoding CD45 (*Ptprc; protein tyrosine phosphatase, receptor type, C*) and of various hematopoietic transcription factors (Runx1, c-Myb, Evi-1, SCL and Gata2) (Figure 3C-H). CD45-negative c-Kit$^+$/CD31$^+$/CD34$^+$ cells expressed low levels of *CD45* mRNA. *Ptprc* transcript levels increased significantly as CD45 surface protein expression was up-regulated in the c-Kit$^+$/CD31$^+$/CD34$^+$ population. Expression levels of all hematopoietic transcription factor genes assayed except *Evi-1* was highest in CD45-low positive c-Kit$^+$/CD31$^+$/CD34$^+$ cells. In agreement with flow cytometric analysis, evaluation of CD45 protein expression by immunohistochemistry indicated that IACs in the OMA at 9.5 dpc were CD45-negative while some IACs in the DA, OMA and UA were CD45-positive by 10.5 dpc (Figure 4A-D).

IAC formation in the developing human embryo is poorly defined. Having defined the developmental progression of IAC in the mouse above, we next examined IAC morphology and phenotype in a 32 day-old human embryo. Immunohistochemistry of embryonic human cryosections was performed using anti-human CD34 and CD45 antibodies. As shown in Figure 4E, IACs can be detected in ventral wall of the dorsal aorta. CD34 was expressed by a wide range of vascular endothelial cells throughout the embryo. CD45 was restricted to round and in many cases clearly circulating cells. However, within the IAC observable on the ventral wall of the dorsal aorta, cells expressing both CD34 and CD45 can be seen. This reflects the expression pattern we have identified in embryonic mouse IACs.

Transcription factor hierarchy in IAC development

We next observed IAC formation by immunohistochemistry and flow cytometry in mouse embryos harboring mutations associated with aberrant embryonic hematopoiesis [27–32]. Immunohistochemical analysis of *Runx1*$^{-/-}$ embryos lacked IACs in the DA, OMA and UA. Flow cytometric analyses confirmed the absence of c-Kit$^+$/CD31$^+$/CD34$^+$ cells in *Runx1*$^{-/-}$ embryos compared to wild type embryos (Figure 5A-B). *Evi-1*$^{-/-}$ embryos also lacked IACs in the DA, OMA and UA by immunohistochemistry. However, a small frequency of c-Kit$^+$/CD31$^+$/CD34$^+$ cells could be detected by flow cytometry (Figure 5C). In *c-Myb*$^{-/-}$ embryos, IACs were observed at the DA, OMA and UA, and c-Kit$^+$/CD31$^+$/CD34$^+$ cells were also observed by flow cytometry (Figure 5D). Collectively, these results demonstrate that Runx1 is essential for IAC formation while Evi-1 appears to be playing a function downstream of Runx1 in this process.

Discussion

During embryogenesis, a unique cell biological shift takes places in which endothelial cells with adherens junctions detach from each other, alter gene expression and become hematopoietic cells. This process is limited both anatomically and temporally. We here demonstrated that the transition from endothelial to hematopoietic phenotype of IACs occurs from 9.5 dpc in the mouse embryo, earlier than previously described. Furthermore, we show that IACs are identifiable in the human embryo based on CD45 expression, implying that this process in mice is applicable to human.

Previously, we reported an immunohistochemistry visualization technique revealing hematopoietic cell clusters in placenta using thick (20 μm) cryo-sections and antibodies recognizing embryonic HSC markers [26]. Here, we applied this technique to obtain high quality confocal images of intra-aortic/arterial clusters (IACs) in the AGM region. We defined IACs as c-Kit$^+$/CD31$^+$/CD34$^+$ cells. Recently, c-Kit$^+$/CD31$^+$/SSEA-1$^-$ cells were also identified in the AGM region [11]. As CD31 is expressed on both IACs and primordial germ cells (PGCs), it was necessary to exclude PGCs according to SSEA-1 expression. As shown in Figure 2 and 5, we

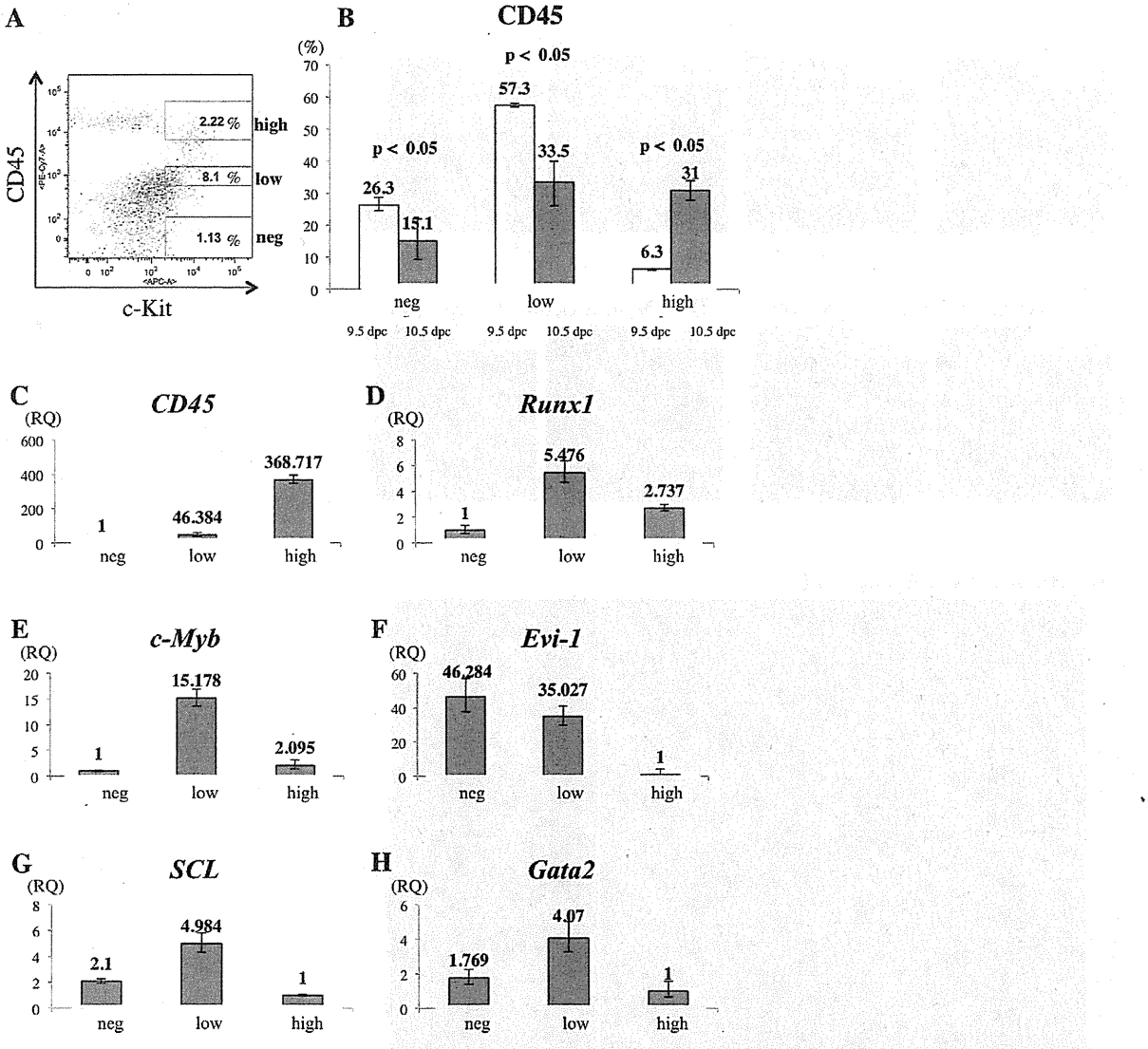

Figure 3. Gene expression analysis in CD31$^+$/CD34$^+$/c-Kit$^+$ AGM cells separated by CD45 expression. (**A**) Single cell suspensions of the caudal portion of embryos containing the AGM region at 10.5 dpc were prepared and analyzed by flow cytometry. Cells expressing CD31 and CD34, IAC markers, were first gated. The profile shows expression of c-Kit (x-axis) and CD45 (y-axis) in CD31$^+$/CD34$^+$ AGM cells (left). Based on intensity of CD45 expression, CD31$^+$/CD34$^+$/c-Kit$^+$ AGM cells were separated into three fractions, CD45-negative (under 10^2 of CD45-fluorescence, same as negative control), -low positive (from $10^{2.5}$ to $10^{3.5}$ of CD45-fluorescence), and -high positive (approximately over 10^4 of CD45-fluorescence). Isotype control and compensation samples of flow cytometric analysis are shown in Figure S4 and S5. (**B**) The percentage of CD45-negative, -low positive, and -high positive c-Kit$^+$/CD31$^+$/CD34$^+$ AGM cells was calculated both at 9.5 dpc (white bars) and 10.5 dpc (black bars). (**C-H**) Gene expression of *CD45* (C), *Runx1* (D), *c-Myb* (E), *Evi-1* (F), *SCL* (G) and *Gata2* (H) was analyzed in sorted CD45-negative, -low positive and -high positive c-Kit$^+$/CD31$^+$/CD34$^+$ AGM cells. Expression levels of *CD45* mRNA are up-regulated as c-Kit$^+$/CD31$^+$/CD34$^+$ cells express CD45 surface protein. Expression levels of *Runx1*, *c-Myb*, *Evi-1*, *SCL* and *Gata2* were highest in CD45-low positive c-Kit$^+$/CD31$^+$/CD34$^+$ cells, whereas that of *Evi-1* was highest in CD45-negative c-Kit$^+$/CD31$^+$/CD34$^+$ cells. RQ represents relative quantity of template in the original sample.
doi:10.1371/journal.pone.0035763.g003

could observe a small number of CD31$^+$/CD34$^-$ cells, which are likely to be PGCs. Since PGCs do not express CD34 at this stage, we could positively select the IAC fraction based on our definition by flow cytometry [33]. Our observation of IACs is compatible with the result showing large IACs were primarily observed in omphalomesentric artery (OMA) and umbilical artery (UA) at 10.5 dpc [11]. In the mouse, IACs protruding into the lumen of arteries were previously reported at 9.5 dpc in studies using microscopy and Tie-2 immunohistochemistry [14,34]. Prior to 9.5 dpc, we identified the first IACs, which formed a spherical structure, in the OMA at 9.0 dpc (Figure 1A). The OMA appears at 8.0 dpc and directly connects with the dorsal aorta (DA). The OMA anastomoses with the DA after 9.5 dpc and loses its connection with the UA by 10.5 dpc [14,35]. Our data (Figure 1E) indicate that IACs are proliferative, based on Ki-67 staining. Taken together, it is likely that the first IACs in the OMA proliferate and are distributed into

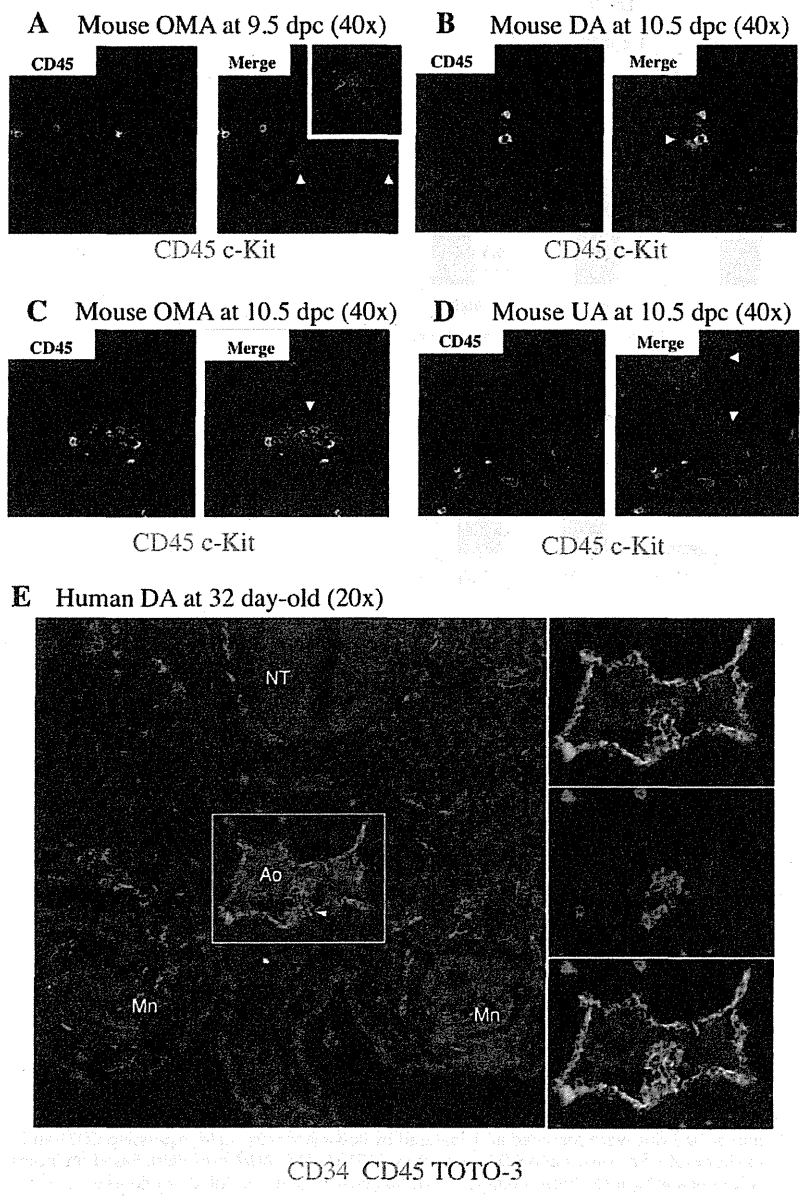

Figure 4. Expression of CD45 by mouse and human IACs. Transverse sections of AGM region were made from ICR mouse embryos at 9.5 and 10.5 dpc and from human embryos at 32 day-old, according to the Carnegie classification, stained with antibodies and observed by confocal microscopy. Arrowheads indicate IACs. (**A**) Mouse IACs in the omphalomesenteric artery (OMA) at 9.5 dpc expressed c-Kit, but not CD45. CD45 (green) and c-Kit (red). Magnified view of IACs is shown at right upper panel in Merge panel. Original magnification is 40x. (**B-D**) Mouse IACs in the dorsal aorta (DA) (B), OMA (C) and umbilical artery (UA) (D) at 10.5 dpc expressed c-Kit, and some expressed CD45. CD45 (green) and c-Kit (red). Original magnification is 40x. (**E**) All human IACs in the DA expressed CD34, and some expressed CD45. CD34 (green), CD45 (red) and TOTO-3 (blue). NT (Neural Tube); Ao (Aorta); Mn (Mesonephros). Original magnification is 20x.
doi:10.1371/journal.pone.0035763.g004

large arteries, such as the DA and UA, as the arterial system develops. Although several reports provide direct evidence that endothelial cells (ECs) generate IACs, we cannot rule out the possibility that either mesodermal cells, the ancestors of hematopoietic cells, or so-called hemangioblasts, which give rise both to ECs and hematopoietic cells, generate IACs by another pathway [17–25]. When VE-cadherin$^+$/CD45$^-$ cells were sorted out from AGM regions at 10.5 dpc, and co-aggregated with OP9 stromal cells, these cells acquired HSC activity [8]. As embryos develop, VE-cadherin$^+$/CD45$^+$ cells from AGM regions at 11.5 dpc can reconstitute adult recipients without culture step, whereas both VE-cadherin$^+$/CD45$^{+/-}$ cells can after aggregation culture with OP9 stromal cells. It suggests that the transition from endothelial to hematopoietic phenotype in pre-HSCs occurs between 10.5 and 11.5 dpc. According to our flow cytometric analysis of IACs, the transition from endothelial to hematopoietic phenotype occurs after 9.5 dpc (Figure 2). Although we found that 33% of c-Kit$^+$/CD31$^+$/CD34$^+$ cells at 9.5 dpc express VE-cadherin, most IACs defined as

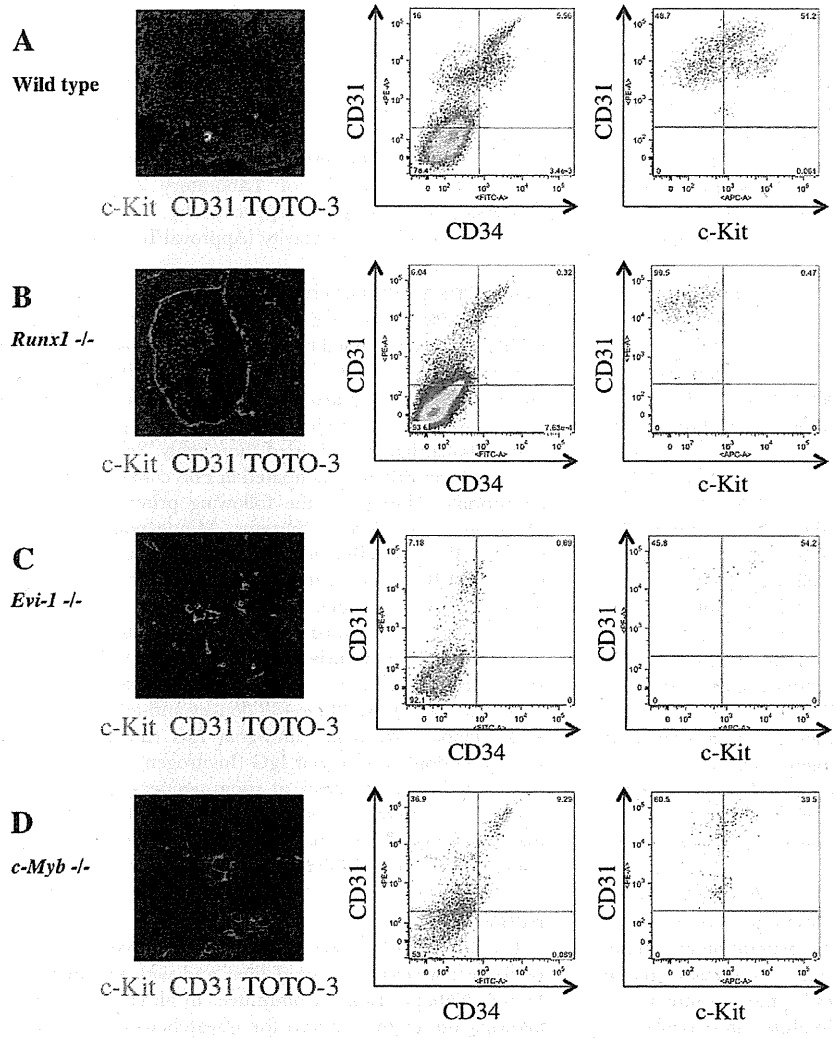

Figure 5. Altered IAC phenotype in *Runx1*$^{-/-}$, *Evi-1*$^{-/-}$ and *c-Myb*$^{-/-}$ embryos. Transverse sections of the AGM region were made from ICR, *Runx1*$^{-/-}$, *Evi-1*$^{-/-}$ and *c-Myb*$^{-/-}$ mouse embryos at 10.5 dpc, stained with antibodies and observed by confocal microscopy. Single cell suspensions of AGM regions from these embryos at 10.5 dpc were prepared and analyzed by flow cytometry. (**A-D**) Left panels show confocal images stained with anti-c-Kit (green) and CD31 (red) antibodies and TOTO-3 (blue). Middle and right panels show flow cytometric profiles of CD34 (x-axis) and CD31 (y-axis), and c-Kit (x-axis) and CD31 (y-axis), respectively. Isotype control and compensation samples of flow cytometric analysis are shown in Figure S2 and S5. (**A**) ICR mouse embryos serve as (wild type) controls. IACs and CD31$^+$/CD34$^+$/c-Kit$^+$ AGM cells were observed. (**B**) No IACs were observed in *Runx1*$^{-/-}$ embryos, whereas the aortic structure was conserved (left). No CD31$^+$/CD34$^+$/c-Kit$^+$ AGM cells were observed, whereas CD31$^+$/CD34$^+$/c-Kit$^-$ AGM cells, which are equivalent to ECs, were observed (middle and right). (**C**) No IACs were observed and aortic structure was altered in *Evi-1*$^{-/-}$ embryos (left). CD31$^+$ AGM cells were observed, but they did not express CD34 and c-Kit (middle and right). (**D**) IACs were observed in *c-Myb*$^{-/-}$ embryos and the aortic structure was conserved (left). CD31$^+$/CD34$^+$/c-Kit$^+$ AGM cells were observed (middle and right).
doi:10.1371/journal.pone.0035763.g005

c-Kit$^+$/CD31$^+$/CD34$^+$ cells by flow cytometry did not contribute to blood vessel structure. VE-cadherin is expressed in IACs as well as in ECs [16]. It is likely that sorted VE-cadherin$^+$/CD45$^-$ cells from AGM regions at 10.5 dpc contained ECs with HSC potential in addition to some IACs. Further studies are necessary to determine how ECs contribute to IAC generation. CD150 belongs to the SLAM family and its expression is developmentally regulated on the surface of HSCs. At 11.5 dpc, CD150$^-$ cells can reconstitute adult recipients, but CD150$^+$ cells not [10]. In this study, CD150 expression was examined on c-Kit$^+$/CD31$^+$/CD34$^+$ cells by flow cytometry and the percentage of CD150 expression was not changed (Figure 2F, H). It will be interesting to compare the CD150 expression between 10.5 and 11.5 dpc.

The pan-leukocyte marker CD45 is a transmembrane glycoprotein that functions as a protein phosphotyrosine phosphatase. Although loss of the *CD45* gene results in T and B lymphocyte anomalies in adult, there appears to be no significant abnormality in HSC development during embryogenesis [36–38]. We observed that CD45 protein expression was up-regulated in c-Kit$^+$/CD31$^+$/CD34$^+$ cells between 9.5 and 10.5 dpc (Figure 2D). Our results are compatible with the report showing that CD45 is expressed on the surface of IACs at 10.5 dpc, but not on the IACs at 9.5 dpc [11].

In agreement with previous reports, we observed no significant differences in HSC activity based on neonatal transplantation, whereas myeloid potential differs based on colony formation assay between CD45-negative and CD45-positive c-Kit$^+$/CD31$^+$/CD34$^+$ cells, suggesting that CD45 expression is not required for hematopoietic cell identity (Figure 2I, J) [39–40]. However, pre-HSCs that can reconstitute both adult and neonatal recipients appear at 10.5 dpc, whereas presumptive ancestor cells of HSC that can reconstitute only neonatal but not adult recipients appear at 9.5 dpc [7,12–13]. In accordance with flow cytometric data, some IACs expressed CD45 while others did not in both 10.5 dpc mouse embryos and 32 day-old human embryos (Figure 4B-E). Taken together, although CD45 does not function in HSC development, its expression on the cell surface might serve as a marker of pre-HSC maturation from ancestor cells of HSC. With regard to myeloid potential, only macrophage development differs (Figure 2I). At 10.5 dpc, macrophages are reportedly c-Kit$^-$/CD31$^-$/CD45$^+$ cells, and we could observe some c-Kit$^-$/CD45$^+$ cells in the AGM regions (Figure 4) [11]. CD45 expression on c-Kit$^+$/CD31$^+$/CD34$^+$ cells might be the diverging point of myeloid potential. Furthermore, we identified *CD45* gene expression in CD45-negative c-Kit$^+$/CD31$^+$/CD34$^+$ cells, suggesting that these cells are primed to differentiate into CD45-positive c-Kit$^+$/CD31$^+$/CD34$^+$ cells. Expression levels of *Runx1, c-Myb, SCL* and *Gata2* were highest in CD45-low positive c-Kit$^+$/CD31$^+$/CD34$^+$ cells, implying that the transition from endothelial to hematopoietic phenotype of IACs occurs in CD45-low positive c-Kit$^+$/CD31$^+$/CD34$^+$ cells, as these transcription factors are reportedly important for the switch to hematopoietic cells [22]. Evi-1 is involved in vasculo-angiogenesis in addition to HSC development [31]. Therefore, high expression level of *Evi-1* gene in CD45-negative c-Kit$^+$/CD31$^+$/CD34$^+$ cells implies that this population still preserves some endothelial identity.

We also investigated IACs from *Runx1*$^{-/-}$, *Evi-1*$^{-/-}$ or *c-Myb*$^{-/-}$ mouse embryos. Runx1 is essential for definitive hematopoiesis, and its expression marks the site of *de novo* generation of definitive hematopoietic cells [28–30]. In agreement with previous reports, we observed an absence of IACs in *Runx1*$^{-/-}$ mouse embryos. *Evi-1*$^{-/-}$ mouse embryos displayed abnormalities in vascular and hematopoietic development [31–32]. As shown in Figure 5C, *Evi-1*$^{-/-}$ mouse embryos comprised a few c-Kit$^+$/CD31$^+$/CD34$^+$ cells based on flow cytometric analysis. High expression of *Evi-1* in CD45-negative c-Kit$^+$/CD31$^+$/CD34$^+$ cells may correlate with vascular development and impairment of IAC formation. c-Myb is essential for HSC maturation and proliferation, and *c-Myb*$^{-/-}$ mouse embryos die at 15.5 dpc from impaired definitive hematopoiesis in fetal liver, although primitive hematopoiesis appears normal [27]. In contrast to *Runx1*$^{-/-}$ or *Evi-1*$^{-/-}$ mouse embryos, *c-Myb*$^{-/-}$ mouse embryos exhibited IACs.

Several evidences reveal that HSCs are generated from ECs [17–21]. Taken together, our results corroborate HSC-generation from ECs and imply that IACs gradually acquire hematopoietic phenotype after 9.5 dpc. Understanding how IACs are generated could lead to an understanding of how to manipulate HSC generation from ES/iPS cells and thus be applicable to future clinical applications.

Materials and Methods

Mice

Ly5.1 (Sankyo Labo Service, Tokyo, Japan) mice, Ly5.2 adult C57/BL6 mice (Kyudo, Tosu, Japan), ICR mice (SLC, Hamamatsu, Japan), *Runx1*$^{+/-}$ mice (provided by Dr. Speck at University of Pennsylvania), *Evi-1*$^{+/-}$ mice (JAX mice and Services, Bar Harbor, ME) and *c-Myb*$^{+/-}$ mice (JAX mice and Services) were used in these studies. To analyze cells, pregnant mice were sacrificed at 9.0–10.5 dpc and somite pair number was counted. Embryos at 9.0 dpc with 12–14 somite pairs (SP), 9.5 dpc with 18–22 SP and 10.5 dpc with 30–34 SP were dissected out, respectively. Animals were handled according to the Guidelines for the Care and Use of Laboratory Animals of Kyushu University. This study was approved by Animal Care and Use Committee, Kyushu University (Approval ID: A21-068-0).

Mouse immunohistochemistry

Embryos were dissected out and fixed in 2% paraformaldehyde in PBS, followed by equilibration in 30% sucrose in PBS. Embryos were embedded in OCT compound (SAKURA, Tokyo, Japan) and frozen in liquid nitrogen. Tissues were sliced at 20 μm on a Leica CM1900 UV cryostat, transferred to glass slides (Matsunami, Osaka, Japan) and dried thoroughly. Sections were blocked in 1% BSA in PBS and incubated in PBS containing 1% BSA with appropriate dilutions of the following primary antibodies: goat anti-mouse c-Kit (R&D Systems, Minneapolis, MN), rat anti-mouse CD31 (BD Biosciences, San Diego, CA), rat anti-mouse CD34 (BD Biosciences), rat anti-mouse CD45 (Biolegend) and rat anti-mouse Ki-67 antigen (Dako Corporation, Carpinteria, CA) at 4C overnight. After washing in PBS three times, sections were incubated with appropriate dilutions of the following secondary antibodies: Alexa Fluor 488 donkey anti-rat IgG (Invitrogen, Carlsbad, CA), Alexa Fluor 488 donkey anti-goat IgG (Invitrogen), Alexa Fluor 546 donkey anti-goat IgG (Invitrogen) and Alexa Fluor 568 donkey anti-goat IgG (Invitrogen), as well as TOTO-3 (Invitrogen) to stain nuclei, at room temperature for 30 minutes. Samples were mounted on coverslips using fluorescent mounting medium (Dako Corporation) and assessed using a FluoView 1000 confocal microscope (Olympus, Tokyo, Japan).

Human tissues

Human embryos were obtained from voluntary abortions performed according to guidelines and with the approval of the French National Ethics Committee. In all cases, written consent allowing use of the embryo for research was obtained from the patient. Developmental age was estimated based on anatomical criteria and the Carnegie classification as previously described [41–42].

Human immunohistochemistry

Embryos were fixed overnight at 4°C in PBS plus 4% paraformaldehyde (Sigma-Aldrich), rinsed twice in PBS, then in PBS/15% sucrose (Sigma-Aldrich) for at least 24 hours. Tissues were then embedded in PBS with 15% sucrose and 7.5% gelatin (Sigma-Aldrich), frozen and stored at -80°C. Frozen sections (5 μm) were stored at −20°C until use, and then thawed and hydrated in PBS [37]. For double-staining, the TSA Plus Fluorescence amplification system was used, according to the manufacturer's instructions (NEN-Perkin Elmer). Endogenous peroxidases were inhibited for 20 minutes in PBS containing 0.2% hydrogen peroxide (Sigma-Aldrich). Sections were washed in PBS and non-specific binding sites were blocked with PBS/5% goat serum (Vector Laboratories) for 1 hour. Sections were then incubated with uncoupled antibody to CD45 (overnight at room temperature). After rinsing, sections were incubated with biotinylated goat anti-mouse IgG antibody (Immunotech) for 1 hour and then with peroxidase-labeled streptavidin (Immunotech) for 1 hour. Staining was revealed using fluorescent tyramide (TMR, Tetramethylrhodamine). Residual peroxidase activity was inhibited in PBS/0.2% hydrogen peroxide for 10 min at RT. After 3

washings. in PBS, slides were treated with an Avidin/Biotin blocking kit according to the manufacturer's instructions (Vector Laboratories). Sections were washed and incubated with anti-CD34 antibody at room temperature for 2 hours, then with biotinylated goat anti-mouse IgG antibody (Immunotech) for 1 hour at RT, and with Alexa 488-labeled streptavidin for 1 hour. Slides were mounted in Vectashield medium (Vector Laboratories). Monoclonal antibodies to CD34 (IgG1, clone Qbend-10) and CD45 (IgG1, clone Hle-1) were purchased from Immunotech and Becton-Dickinson Biosciences, respectively.

Cell preparation

The caudal portion of embryos containing the p-Sp/AGM region was used to obtain a single cell suspension. Tissues were incubated with 1 mg/ml collagenase in medium supplemented with 10% fetal bovine serum for 30 minutes at 37°C and filtered through 40-μm nylon cell strainers (BD Biosciences).

Flow cytometry and cell sorting

Antibodies used for analysis were: FITC-conjugated anti-mouse CD41 (eBioscience, San Diego, CA), FITC-conjugated anti-mouse Sca-1 (eBioscience), FITC-conjugated anti-mouse EPCR (Endothelial Protein C Receptor) known as CD201 (Stem Cell Technologies inc, Vancouver, BC), PE-conjugated anti-mouse CD31 (BD Biosciences), PE-Cy7-conjugated anti-mouse CD45 (BioLegend), APC and APC-Cy7-conjugated anti-mouse c-Kit (BD Biosciences), Aexa Fluor488-conjugated anti-mouse CD150 (BioLegend), APC-conjugated anti-mouse VE-cadherin (clone name; VECD-1, provided by Dr. Ogawa at Kumamoto University), and FITC and Pacific Blue-conjugated anti-mouse CD34 (eBioscience). Flow cytometric analysis and cell sorting were carried out using a FACSAria SORP cell sorter (BDIS, San Jose, CA). Data files were analyzed using FlowJo software (Tree Star, Inc., San Carlos, CA).

RNA extraction and real-time PCR analysis

Total RNA was isolated using the RNAqueous 4PCR kit (Ambion Inc., Austin, Texas). mRNA was reverse transcribed using a High-Capacity RNA-to-cDNA kit (Life Technologies, Carlsbad, CA). The quality of cDNA synthesis was evaluated by amplifying mouse ß-actin using PCR. Thirty thermal cycles were used as follows: denaturation at 95°C for 10 sec, annealing at 60°C for 20 sec, followed by extension at 72°C for 20 seconds. Gene expression levels were measured by real time PCR with TaqMan® Gene Expression Master Mix and StepOnePlus™ real time PCR (Life Technologies). All probes were from TaqMan® Gene Expression Assays (Life Technologies). All analyses were performed in triplicate wells; mRNA levels were normalized to ß-actin and the relative quantity (RQ) of expression was compared with a reference sample.

Colony formation assay

Sorted cells were suspended in 3 ml of MethoCult® GF M3434 (Stemcell Technologies) distributed into three 35 mm dishes and then incubated in 5% CO_2 at 37°C. Colonies were counted up 14 days later using an inverted phase contrast microscope CKX41 (Olympus, Tokyo, Japan).

Transplantation assay

To examine neonatal repopulating HSCs, sorted cells were transplanted into busulfan-treated Ly5.1 mouse neonates as described previously [9,15]. Briefly, time-pregnant mice were injected on days 17 and 18 after conception with 15 μg of busulfan/gram body weight of the mother (Sigma-Aldrich, St.Louis MO). Isolated cells were suspended in 25 μl PBS and transplanted into neonates at the time of delivery using a 100 μl Hamilton syringe (Hamilton, Reno, NV). Approximately one year after transplantation, blood samples were collected, lysed in BD Pharm Lyse (BD Biosciences) and analyzed for CD45.2 expression by flow cytometry.

Supporting Information

Figure S1 Additional confocal images of IAC expressing CD31/CD34/c-Kit in the dorsal aorta of AGM region at 10.5 dpc. Staining for CD34 (red), c-Kit (green), and TOTO-3 (blue) is shown. Original magnification is 40x.
(TIFF)

Figure S2 Single cell suspensions of the caudal portion of embryos containing the p-Sp/AGM region at 9.5 and 10.5 dpc were prepared and analyzed by flow cytometry. Upper panels show isotype control of analysis corresponding to Figure 2A. Lower panels show isotype control of analysis corresponding to Figure 5.
(TIFF)

Figure S3 50–100 sorted $CD31^-/CD34^+/c\text{-}Kit^+$ cells at 9.5 dpc, as well as CD45-negative and CD45-positive $CD31^+/CD34^+/c\text{-}Kit^+$ cells were transplanted into busulfan-treated Ly5.1 mouse neonates. Approximately one year after transplantation, blood samples were collected, lysed in lysing solution and analyzed for CD45.2 expression by flow cytometry. Representative profile of flow cytometric analysis is shown.
(TIFF)

Figure S4 Single cell suspensions of the caudal portion of embryos containing the AGM region at 10.5 dpc were prepared and analyzed by flow cytometry. The profile shows isotype control of analysis corresponding to Figure 3A. Based on the isotype control, sorting gates are set into three fractions, CD45-negative (under 10^2 of CD45-fluorescence, same as negative control), -low positive (from $10^{2.5}$ to $10^{3.5}$ of CD45-fluorescence), and -high positive (approximately over 10^4 of CD45-fluorescence).
(TIFF)

Figure S5 Single cell suspensions of the caudal portion of embryos containing the p-Sp/AGM region at 9.5 and 10.5 dpc were prepared and analyzed by flow cytometry. Compensation samples of analysis corresponding to Figure 3A and 5 were shown.
(TIFF)

Figure S6 Negative and positive controls to transplantation analysis are shown corresponding to Figure S3. Peripheral blood samples were obtained from Ly5.1 adult mouse for negative control and Ly5.2 adult C57/BL6 mice for positive control, respectively.
(TIFF)

Acknowledgments

We thank the Research Support Center, the Graduate School of Medical Sciences, Kyushu University for technical support, Drs. K. Nakao and K. Kulkeaw for technical support, and Dr. Elise Lamar for critical reading of our manuscript.

Author Contributions

Conceived and designed the experiments: DS. Performed the experiments: CM KB YH YK MT DS. Analyzed the data: CM SF KB MT DS. Contributed reagents/materials/analysis tools: CM KB MT KT KA DS. Wrote the paper: CM SF DS.

References

1. Dzierzak E, Speck NA (2008) Of lineage and legacy: the development of mammalian hematopoietic stem cells. Nat Immunol 9: 129–136.
2. Mikkola HK, Orkin SH (2006) The journey of developing hematopoietic stem cells. Development 133: 3733–3744.
3. Godin I, Cumano A (2002) The hare and the tortoise: an embryonic haematopoietic race. Nat Rev Immunol 2: 593–604.
4. Dieterlen-Lievre F, Pouget C, Bollerot K, Jaffredo T (2006) Are intra-aortic hemopoietic cells derived from endothelial cells during ontogeny? Trends Cardiovasc Med 16: 128–139.
5. Jaffredo T, Bollerot K, Sugiyama D, Gautier R, Drevon C (2005) Tracing the hemangioblast during embryogenesis: developmental relationships between endothelial and hematopoietic cells. Int J Dev Biol 49: 269–277.
6. Sugiyama D, Tsuji K (2006) Definitive hematopoiesis from endothelial cells in the mouse embryo; a simple guide. Trends Cardiovasc Med 16: 45–49.
7. Medvinsky A, Dzierzak E (1996) Definitive hematopoiesis is autonomously initiated by the AGM region. Cell 86: 897–906.
8. Taoudi S, Gonneau C, Moore K, Sheridan JM, Blackburn CC, et al. (2008) Extensive hematopoietic stem cell generation in the AGM region via maturation of VE-cadherin+CD45+ pre-definitive HSCs. Cell Stem Cell 3: 99–108.
9. Rybtsov S, Sobiesiak M, Taoudi S, Souilhol C, Senserrich J, et al. (2011) Hierarchical organization and early hematopoietic specification of the developing HSC lineage in the AGM region. J Exp Med 208: 1305–1315.
10. McKinney-Freeman SL, Naveiras O, Yates F, Loewer S, Philitas M, et al. (2009) Surface antigen phenotypes of hematopoietic stem cells from embryos and murine embryonic stem cells. Blood 114: 268–278.
11. Yokomizo T, Dzierzak E (2010) Three-dimensional cartography of hematopoietic clusters in the vasculature of whole mouse embryos. Development 137: 3651–3661.
12. Kumano K, Chiba S, Kunisato A, Sata M, Saito T, et al. (2003) Notch1 but not Notch2 is essential for generating hematopoietic stem cells from endothelial cells. Immunity 18: 699–711.
13. Yoder MC, Hiatt K, Dutt P, Mukherjee P, Bodine DM, et al. (1997) Characterization of definitive lymphohematopoietic stem cells in the day 9 murine yolk sac. Immunity 7: 335–344.
14. Garcia-Porrero JA, Godin IE, Dieterlen-Lievre F (1995) Potential intraembryonic hemogenic sites at pre-liver stages in the mouse. Anat Embryol (Berl) 192: 425–435.
15. Garcia-Porrero JA, Manaia A, Jimeno J, Lasky LL, Dieterlen-Lievre F, et al. (1998) Antigenic profiles of endothelial and hemopoietic lineages in murine intraembryonic hemogenic sites. Dev Comp Immunol 22: 303–319.
16. Fraser ST, Ogawa M, Yokomizo T, Ito Y, Nishikawa S (2003) Putative intermediate precursor between hematogenic endothelial cells and blood cells in the developing embryo. Dev Growth Differ 45: 63–75.
17. Jaffredo T, Gautier R, Eichmann A, Dieterlen-Lievre F (1998) Intraaortic hemopoietic cells are derived from endothelial cells during ontogeny. Development 125: 4575–4583.
18. Sugiyama D, Ogawa M, Hirose I, Jaffredo T, Arai K, et al. (2003) Erythropoiesis from acetyl LDL incorporating endothelial cells at the preliver stage. Blood 101: 4733–4738.
19. Sugiyama D, Arai K, Tsuji K (2005) Definitive hematopoiesis from acetyl LDL incorporating endothelial cells in the mouse embryo. Stem Cells Dev 14: 687–696.
20. Bertrand JY, Giroux S, Golub R, Klaine M, Jalil A, et al. (2005) Characterization of purified intraembryonic hematopoietic stem cells as a tool to define their site of origin. Proc Natl Acad Sci U S A 102: 134–139.
21. Zovein AC, Hofmann JJ, Lynch M, French WJ, Turlo KA, et al. (2008) Fate tracing reveals the endothelial origin of hematopoietic stem cells. Cell Stem Cell 3: 625–636.
22. Chen MJ, Yokomizo T, Zeigler BM, Dzierzak E, Speck NA (2009) Runx1 is required for the endothelial to haematopoietic cell transition but not thereafter. Nature 457: 887–891.
23. Bertrand JY, Chi NC, Santoso B, Teng S, Stainier DY, et al. (2010) Haematopoietic stem cells derive directly from aortic endothelium during development. Nature 464: 108–111.
24. Kissa K, Herbomel P (2010) Blood stem cells emerge from aortic endothelium by a novel type of cell transition. Nature 464: 112–115.
25. Boisset JC, van Cappellen W, Andrieu-Soler C, Galjart N, Dzierzak E, et al. (2010) In vivo imaging of haematopoietic cells emerging from the mouse aortic endothelium. Nature 464: 116–120.
26. Sasaki T, Mizuochi C, Horio Y, Nakao K, Akashi K, et al. (2010) Regulation of hematopoietic cell clusters in the placental niche through SCF/Kit signaling in embryonic mouse. Development 137: 3941–3952.
27. Mucenski ML, McLain K, Kier AB, Swerdlow SH, Schreiner CM, et al. (1991) A functional c-myb gene is required for normal murine fetal hepatic hematopoiesis. Cell 65: 677–689.
28. Okuda T, van Deursen J, Hiebert SW, Grosveld G, Downing JR (1996) AML1, the target of multiple chromosomal translocations in human leukemia, is essential for normal fetal liver hematopoiesis. Cell 84: 321–330.
29. Wang Q, Stacy T, Binder M, Marin-Padilla M, Sharpe AH, et al. (1996) Disruption of the Cbfa2 gene causes necrosis and hemorrhaging in the central nervous system and blocks definitive hematopoiesis. Proc Natl Acad Sci U S A 93: 3444–3449.
30. North T, Gu TL, Stacy T, Wang Q, Howard L, et al. (1999) Cbfa2 is required for the formation of intra-aortic hematopoietic clusters. Development 126: 2563–2575.
31. Yuasa H, Oike Y, Iwama A, Nishikata I, Sugiyama D, et al. (2005) Oncogenic transcription factor Evi1 regulates hematopoietic stem cell proliferation through GATA-2 expression. EMBO J 24: 1976–1987.
32. Goyama S, Yamamoto G, Shimabe M, Sato T, Ichikawa M, et al. (2008) Evi-1 is a critical regulator for hematopoietic stem cells and transformed leukemic cells. Cell Stem Cell 3: 207–220.
33. Wood HB, May G, Healy L, Enver T, Morris-Kay GM (1997) CD34 expression patterns during early mouse development are related to modes of blood vessel formation and reveal additional sites of hematopoiesis. Blood 90: 2300–2311.
34. Takakura N, Huang XL, Naruse T, Hamaguchi I, Dumont DJ, et al. (1998) Critical role of the TIE2 endothelial cell receptor in the development of definitive hematopoiesis. Immunity 9: 677–686.
35. Theiler K (1972) The house mouse: development and normal stages from fertilization to 4 weeks of age. Springer, Berlin Heidelberg New York.
36. Kishihara K, Penninger J, Wallace VA, Kundig TM, Kawai K, et al. (1993) Normal B lymphocyte development but impaired T cell maturation in CD45-exon6 protein tyrosine phosphatase-deficient mice. Cell 74: 143–156.
37. Byth KF, Conroy LA, Howlett S, Smith AJ, May J, et al. (1996) CD45-null transgenic mice reveal a positive regulatory role for CD45 in early thymocyte development, in the selection of CD4+CD8+ thymocytes, and B cell maturation. J Exp Med 183: 1707–1718.
38. Mee PJ, Turner M, Basson MA, Costello PS, Zamoyska R, et al. (1999) Greatly reduced efficiency of both positive and negative selection of thymocytes in CD45 tyrosine phosphatase-deficient mice. Eur J Immunol 29: 2923–2933.
39. North TE, de Bruijn MF, Stacy T, Talebian L, Lind E, et al. (2002) Runx1 expression marks long-term repopulating hematopoietic stem cells in the midgestation mouse embryo. Immunity 16: 661–672.
40. Matsubara A, Iwama A, Yamazaki S, Furuta C, Hirasawa R, et al. (2005) Endomucin, a CD34-like sialomucin, marks hematopoietic stem cells throughout development. J Exp Med 202: 1483–1492.
41. O'Rahilly R, Muller F (1987) Development Stages in Human Embryos. Washington: Carnegie Institution of Washington.
42. Tavian M, Peault B (2005) The changing cellular environments of hematopoiesis in human development in utero. Exp Hematol 33: 1062–1069.

Cell Biology International

Cell Biol. Int. (2012) 36, 195–202 (Printed in Great Britain)

Research Article

Ectopic expression of Hmgn2 antagonizes mouse erythroid differentiation *in vitro*

Kasem Kulkeaw*, Tomoko Inoue*,†, Chiyo Mizuochi*, Yuka Horio*, Yasushi Ishihama‡ and Daisuke Sugiyama[1]*

* Advanced Medical Initiatives, Division of Hematopoietic Stem Cells, Department of Advanced Medical Initiatives, Faculty of Medical Sciences, Kyushu University, Fukuoka, 812-8582, Japan

† Department of Molecular Genetics, Medical Institute of Bioregulation, Kyushu University, Fukuoka, 812-8582, Japan

‡ Graduate School of Pharmaceutical Sciences, Kyoto University, Kyoto, 606-8501, Japan

Abstract

Hmgn2 (high mobility group nucleosomal 2), a ubiquitous nucleosome-binding protein that unfolds chromatin fibres and enhances DNA replication, reportedly regulates differentiation of epithelial and mesenchymal cells. To investigate how Hmgn2 regulates HC (haemopoietic cell) differentiation, we quantified *Hmgn2* expression in HCs of mouse FL (fetal liver) during erythroid differentiation. *Hmgn2* expression levels were >10-fold higher in immature erythroid progenitors than in mature erythroid cells, suggesting that Hmgn2 antagonizes erythroid differentiation. To address this issue, *Hmgn2* were transfected into both Friend erythroleukaemia cells and FL HCs. There was a 3.3-fold decrease in relatively mature c-Kit$^+$/CD71$^+$ erythroid cells, a 2.9-fold increase in immature c-Kit$^+$/CD71$^-$ erythroid cells in transfected Friend cells, a 1.1-fold decrease in relatively mature CD71$^+$/Ter119$^+$ erythroid cells, and a 1.7-fold increase in relatively immature c-Kit$^+$/CD71$^+$ erythroid cells in FL HCs accompanied by down-regulation of genes encoding the erythroid transcription factors, Gata1 and Klf1. Two days after *Hmgn2* transfection of Friend erythroleukaemia cells, the number of S-phase cells increased, whereas the number of cells in G_1 decreased, while that of mitotic cells remained unchanged. We conclude that ectopic expression of Hmgn2 antagonizes mouse erythroid differentiation *in vitro*, which may be due to enhancement of DNA replication and/or blocking entry of mitosis at S-phase.

Keywords: erythroid differentiation; erythroleukaemia cell; fetal liver; Hmgn2

1. Introduction

Hmgn (high mobility group nucleosomal)-binding proteins constitute a family of ubiquitous nuclear proteins comprising Hmgn1–Hmgn4 and NSBP1 (nucleosomal binding protein 1). Hmgn1 and Hmgn2 are widely expressed, whereas the remaining family members have a more tissue-specific expression pattern (Bustin 1999, 2001). Nuclear Hmgn1 and Hmgn2, which are 53% homologous, constitute approximately 10% of all nuclear protein in mice (Bustin and Reeves, 1996). Both bind to nucleosomes as a homodimer. The NBD (nucleosome-binding domain) binds to the 147 bp nucleosome core particle rather than to a specific DNA sequence (Shirakawa et al., 2000; Ueda et al., 2008), while the CHUD (chromatin-unfolding domain) reduces compactness of the chromatin fibre (Bustin, 2001). Hmgn2 facilitates accessibility of transcription factors and the replication machinery to chromatin, thereby enhancing transcription (Trieschmann et al., 1995a, 1995b) and DNA replication (Vestner et al., 1998). In addition to nucleosome binding, Hmgn2 also modulates DNA binding of homeodomain transcription factors (Amen et al., 2008). At the 2-cell stage in mouse embryos, *Hmgn2* knockdown by antisense oligonucleotide delays cell division (Mohamed et al., 2001). *Hmgn2* expression is also down-regulated during differentiation of osteoblasts in mouse embryos (Shakoori et al., 1993). However, Hmgn2 is highly expressed in cells undergoing differentiation, such as the basal layer of epithelial cells in *Xenopus laevis* (Korner et al., 2003) and mesenchymal-to-epithelial transitions in the mouse kidney (Lehtonen and Lehtonen, 2001).

Haematopoiesis is the process in which HSCs (haemopoietic stem cells) are generated, differentiate into specific progenitors and mature into various blood cell types, such as erythrocytes, megakaryocytes, lymphocytes, neutrophils and macrophages (Weissman, 2000). Erythropoiesis is the process by which a large number of enucleated erythrocytes are produced from HSCs (McGrath and Palis, 2008). During embryogenesis, the FL (fetal liver) is a major organ of HSC expansion and erythrocyte production (Ema and Nakauchi, 2000; Sugiyama and Tsuji, 2006). Erythropoiesis shifts to BM (bone marrow) shortly before birth (Dzierzak et al., 1998). During erythroid differentiation, erythroblasts lose their capacity to proliferate and leave the cell cycle (Buttitta and Edgar, 2007). However, molecular mechanisms underlying erythroid differentiation have not been fully elucidated.

We have focused on the role of Hmgn2 in erythroid differentiation in mice. By assessing the differentiation status of erythroid cells by flow cytometry and gene expression after

[1]To whom correspondence should be addressed (email ds-mons@yb3.so-net.ne.jp).

Abbreviations: AcGFP, *Aequorea coerulescens* green fluorescent protein; APC, allophycocyanin; BFU-E, burst-forming unit-erythroid; CFU-E, colony-forming unit-erythroid; CHUD, chromatin-unfolding domain; dpc, day post coitum; EPO, erythropoietin; FBS, fetal bovine serum; FL, fetal liver; GFP, green fluorescent protein; HC, haemopoietic cell; Hmgn, high mobility group nucleosomal; HSC, haemopoietic stem cell; IL-3, interleukin 3; IRES, internal ribosome entry site; α-MEM, α-minimum essential medium; MNC, mononuclear cell; NBD, nucleosome-binding domain; NLS, nuclear localization signal; PE, phycoerythrin; PI, propidium iodide; PBSBA, BSA in PBS; RQ, relative quantity; RT–PCR, reverse transcription–PCR; Sca-1, stem cell antigen-1; SCF, stem cell factor; TBS-T, TBS containing 0.1% Tween-20; TPO, thrombopoietin; WB, Western blot.